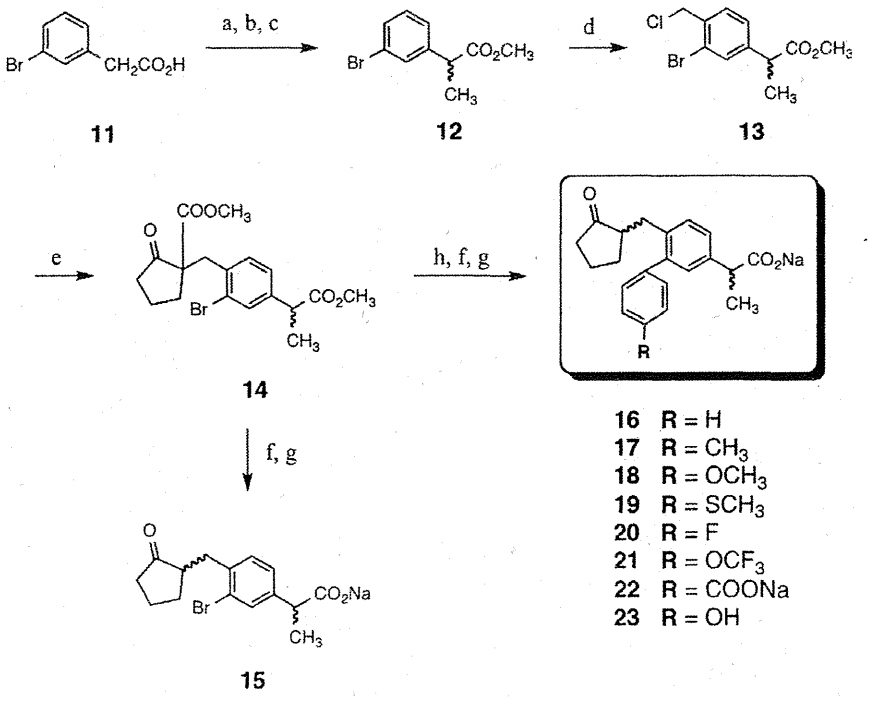

Scheme 2. Synthesis of loxoprofen derivatives with modification at the 3-position of the phenyl ring by Br (**15**) and a *para*-substituted aryl group (**16–23**). Reagents and conditions: (a) MeOH, HCl, reflux; (b) LDA, THF, −78 °C; (c) CH_3I, −78 to −50 °C; (d) $AlCl_3$, $SnCl_4$, 1,3-dioxolane, CH_3OCH_2Cl, 0 °C to rt; (e) methyl 2-oxyocyclopentanecarboxylate, K_2CO_3, acetone, reflux; (f) AcOH, HCL, reflux; (g) 1 M NaOH aq, C_2H_5OH, reflux; (h) R-C6H4-B(OH)2, $PD(PPh_3)_4$, Na_2CO_3, THF, reflux.

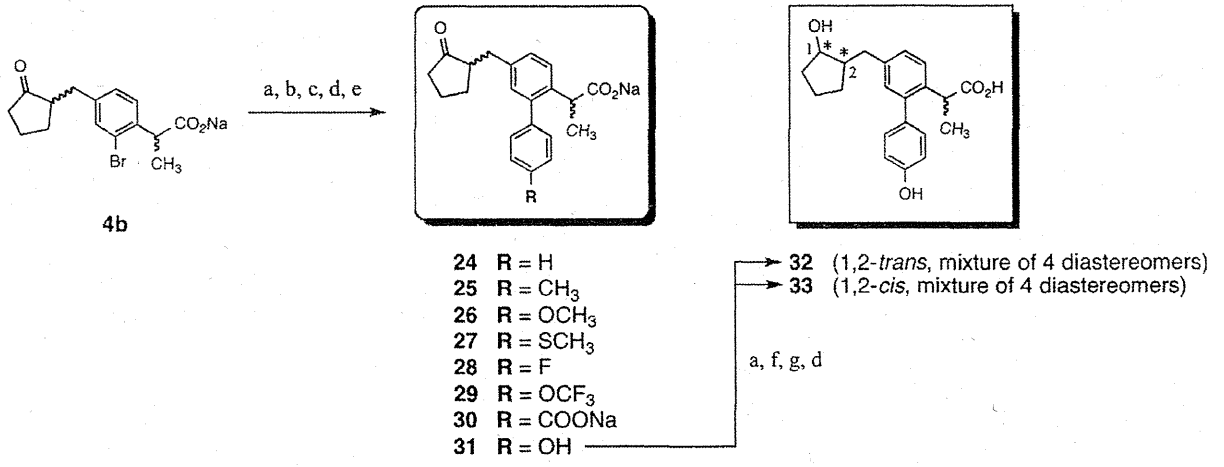

Scheme 3. Synthesis of loxoprofen derivatives with modification at the 2-position of the phenyl ring by a *para*-substituted aryl group (**24–33**). Reagents and conditions: (a) 6 M HCL aq, CH_2Cl_2; (c) R-C6H4-B(OH)2, $PD(PPh_3)_4$, Na_2CO_3, THF, reflux; (d) KOH, C_2H_5OH, H_2O, reflux; (e) 1 M NaOH, C_2H_5OH, reflux; (f) 4-DMAP, EDC, CH_2OH; (g) $NaBH_4$, C_2H_5OH.

followed by acidification. Finally, the carboxylic acid group was transformed into the sodium salt by treatment with NaOH to yield target compounds **24–31**.

The reduction products of **31**, *trans*-alcohol **32** and *cis*-alcohol **33** were prepared by treatment of the methyl ester intermediate of **31** with sodium borohydride ($NaBH_4$) followed by alkaline hydrolysis. The structures of **32** and **33** were identified based on the characteristic NMR signal of the proton on the asymmetric carbon attached to the hydroxyl group.

All target compounds were pure and stable. The final compounds were characterized by ^1H NMR, ^{13}C NMR, infrared spectroscopy (IR), high resolution mass spectra (HR-MS) and elemental analysis.

3. Results and discussion

We have employed loxoprofen sodium **1** (Fig. 1) as a lead compound to obtain NSAIDs with lower membrane permeabilization activity or higher COX-2 specificity. On this basis we synthesized a series of derivatives of **1** by modification of the phenyl ring with electron withdrawing groups such as halogens or modified phenyl

rings. We previously reported that two of the compounds, 2-fluoroloxoprofen **4a** and 2-bromoloxoprofen **4b** (Fig. 1), have lower membrane permeabilization activity than **1**.[25] In this study, we examined the membrane permeabilization activities and inhibitory effects on COX-1 and COX-2 of other derivatives to find other valuable compounds, such as those with COX-2 specificity.

We previously established an assay system for assessing the membrane permeabilization activity of NSAIDs, using calcein-loaded liposomes. Calcein fluorescence is very weak at high concentrations due to self-quenching, so the addition of membrane-permeabilizing drugs to a medium containing calcein-loaded liposomes causes an increase in fluorescence by diluting the calcein.[14] In this study, we used the EC_{50} index, defined as the concentration of each compound required for 50% release of calcein.

Table 1 shows the membrane permeabilization activities and inhibitory effects on COX-1 and COX-2 of loxoprofen derivatives with modification at the 3- or 2-position of the phenyl ring by halogens and the nitro group. The inhibitory effect on COX-1 and COX-2 is shown as the IC_{50} index, defined as the concentration of each compound required for 50% inhibition of each form of COX. Compared to **1**, 4a and **4b**, 2-chloroloxoprofen **10a** and 2-iodoloxoprofen **10b** showed higher membrane permeabilization activity, thus demonstrating that the species of halogen introduced to **1** is an important determinant of the membrane permeabilization activity. We also found that 3-bromoloxoprofen **15** has much higher membrane permeabilization activity than **4b** (Table 1), showing that the modification position on the phenyl ring is also important. Furthermore, we found that 2-nitroloxoprofen **10c** has lower membrane permeabilization activity and a lower inhibitory effect on COX-1 and COX-2 than **1** (Table 1).

The orientation of the active metabolite of **1** and interaction between the compound and amino acid residues in the active site of COX-1 or COX-2 were examined by molecular modeling and docking studies. As shown in Fig. 2, the cyclopentanone ring interacts with Y385 and S530, whereas propanoic acid interacts with R120 and Y355. All of these amino acids were reported to be important for the interaction between COXs and NSAIDs.[28–31] It is also well known that COX-2 has a side pocket[28,32] (Fig. 2). Thus, it could be predicted that introduction of a bulky functional group into the 3- or 2-position of the phenyl ring of **1** results in an increase in its specificity for COX-2 over COX-1. Therefore, we synthesized loxoprofen derivatives with modification at the 3- or 2-position of the phenyl ring by para-substituted aryl groups.

Table 2 shows the membrane permeabilization activities and inhibitory effects on COX-1 and COX-2 of these derivatives, indicating the importance of the modification position of the phenyl ring (3- or 2-position) for determining membrane permeabilization activity and inhibitory effect on COX-1 and COX-2. For example, the membrane permeabilization activity and inhibitory effects on COX-1 and COX-2 of **31** were much higher than those of **23** (Table 2) and we have no clear explanation for this difference. All derivatives except **23** showed higher membrane permeabilization activity than **1**. On the other hand, none of these derivatives showed a more potent inhibitory activity on COX-1 and COX-2 than **1**. Among these derivatives, 2-{4′-hydroxy-5-[(2-oxocyclopentyl)methyl]biphenyl-2-yl}propanoate 31 showed the most potent inhibitory effect on COX-2 and the highest specificity for COX-2 over COX-1; the extent of this specificity is similar to that of celecoxib (Table 2). The combined results show that **31** is a loxoprofen derivative with higher membrane permeabilization activity, a similar inhibitory effect on COX-2, and a higher specificity for COX-2, compared to **1**. On this basis we selected this compound for further investigation (see below).

As described above, **1** is a pro-drug and the *trans*-alcohol derivative is the active metabolite. In order to test whether or not **31** maintains this characteristic, we examined the COX-inhibitory activity of the *trans*- and *cis*-alcohol forms of **31** (**32** and **33**, respectively). The *trans*-alcohol derivative of **1** (**2**, Fig. 1) showed a more potent inhibitory effect on both COX-1 and COX-2 than **1** or its *cis*-alcohol derivative (**3**, Fig. 1) (Table 2). In contrast to the case of **1**, the inhibitory effect on COX-2 was similar between **31**, 32 and **33** (Table 2). Furthermore, the inhibitory effect of **32** on COX-1 was less than that of **33** (Table 1). These results suggest that **31** does not retain the pro-drug characteristic of **1**.

We then evaluated the activity of **31** in vivo. Compound **1** (40 or 50 mg/kg) and equivalent molar amounts of **31** were orally administered to rats and the lesion index was calculated (see Section 5.5). Administration of **1** produced gastric lesions in a dose-dependent manner (Fig. 3), as described previously.[21,22] In contrast, production of gastric lesions was not detected after oral administration of **31** (Fig. 3). We also measured the gastric level of PGE_2 by enzyme immunoassay (EIA) after oral administration of these compounds. As shown in Fig. 3B, the administration of **31** decreased the level of PGE_2, albeit to an extent less than that seen with **1**. Considering our hypothesis that both a decrease in the gastric level of PGE_2 and an increase in gastric mucosal damage due to membrane permeabilization activity of NSAIDs are involved in the production of NSAID-induced gastric lesions, the lower lesion-producing activity of **31** seems to be due to its selectivity for COX-2, resulting in less activity for decreasing the gastric level of PGE_2.

Finally, we compared the anti-inflammatory effects of **31** to **1** by employing a rat carrageenan-induced footpad edema assay. As shown in Fig. 4A, the volume of edema was significantly decreased after oral administration of **1**, confirming it's previously described anti-inflammatory activity.[23,33] The effects of **31** were mostly the same as that of **1** (Fig. 4A). We also found that the level of PGE_2 associated with the footpad edema decreased after oral administration of **31** and the extent was similar to that seen with **1** (Fig. 4B). These results show that **31** has an anti-inflammatory activity equivalent to **1**. This finding may be related to the

Table 1
In vitro membrane permeabilization assay and human whole blood assay for inhibition of COX-1- and COX-2-derived PG biosynthesis; loxoprofen derivatives with modification at the 3- or 2-position of the phenyl ring by halogens and the nitro group

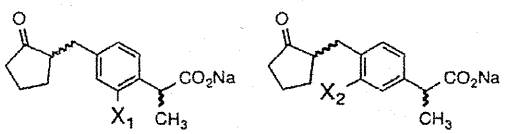

Compounds	X_1 or X_2	EC_{50} (mM)	IC_{50} (μM)		COX-1/COX-2
		Calcein release	COX-1	COX-2	
1		800[a]	24[a]	10[a]	2.5[a]
4a	X_1 = F	>1000[a]	24[a]	14[a]	0.2[a]
4b	X_1 = Br	>1000[a]	30[a]	65[a]	0.1[a]
10a	X_1 = Cl	100	4	2	1.8
10b	X_1 = I	150	270	540	0.5
10c	X_1 = NO_2	>1000	93	49	1.9
15	X_2 = Br	<100	49	23	2.1

Calcein-loaded liposomes were incubated with each compound. The release of calcein from the liposomes was determined by measuring fluorescence intensity. Triton X-100 (10 μM) was used to establish the 100% level of membrane permeabilization. EC_{50} value (concentration of each compound required for 50% release of calcein) is shown.

The inhibitory effect of each compound on COX-1- and COX-2-derived PG biosynthesis was measured and the IC_{50} value (concentration of each compound required for 50% inhibition) and the COX-1/COX-2 ratio of IC_{50} value are shown. The values of IC_{50} were estimated from the sigmoid-like dose–response curve (4-parameter logistic curve model) drawn by the logistic-curve fitting software (ImageJ 1.43u; National Institutes of Health, USA). Mean values are presented (n = 3).

[a] Data from our previous report.[25]

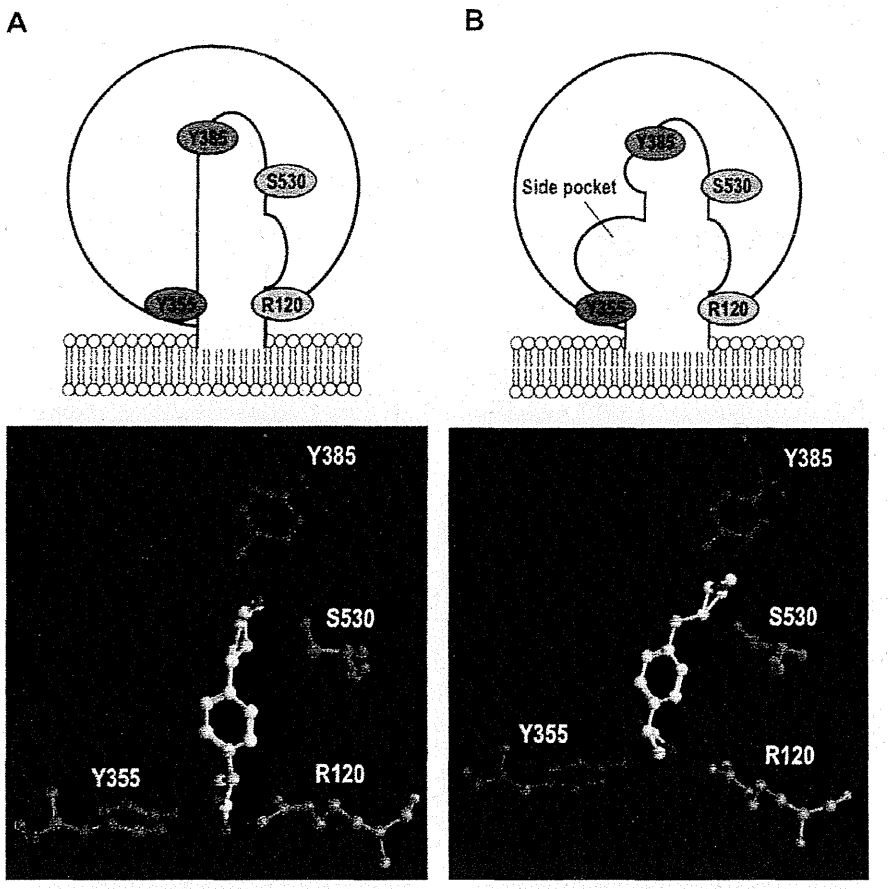

Figure 2. Potential binding mode of (*S*)-2-{4-[((1*R*, 2*S*)-2-hydroxycyclopentyl)methyl]phenyl}propanoic acid to the active site of sheep COX-1 (A) or murine COX-2 (B). Hydrogen atoms of the amino acid residues and the ligand have been removed.

in vitro observation that the inhibitory effect of **1** on COX-2 was indistinguishable from that of **31** (Table 2).

The inhibitory activity of **31** on COX-2 was much higher than that of **23** (Table 2), indicating the importance of the modification position of the phenyl ring (3- or 2-position) for determining the inhibitory effect on COX-2. Thus, we compared the interaction with COX-2 between **23** and **31** by molecular modeling and docking studies. The interaction between the cyclopentanone ring with Y385 and S530 and propanoic acid with R120 and Y355 was similar between **31** (Fig. 5B) and the active metabolite of **1** (Fig. 2B). Furthermore, the introduced phenyl ring of **31** interacts with some amino acids (H90, R513, F518 and V523) (Fig. 5B), which are reported to be located in the side pocket of COX-2.[34,35] On the other hand, molecular modeling and docking studies suggested that the interaction between the cyclopentanone ring with Y385 and S530 and propanoic acid with R120 and Y355 was not possible for **23** (Fig. 5A). As a result, lowest U_{total} index is calculated to be 59.2 and 29.5 kcal/mol for **23** and **31**, respectively; the lower lowest U_{total} index means the higher interaction of two molecules.[36]

A recently raised issue concerning the use of selective COX-2 inhibitors is their potential risk for cardiovascular thrombotic events.[8,9] This may be due to the fact that prostacyclin, a potent anti-aggregator of platelets and a vasodilator, is mainly produced by COX-2 in vascular endothelial cells, while thromboxane A_2, a potent aggregator of platelets and a vasoconstrictor, is mainly produced by COX-1 in platelets.[37–39] Because of this concern, rofecoxib and valdecoxib were withdrawn from the worldwide market.[8,10] On the other hand, it is not clear whether or not celecoxib use is a potential risk factor for cardiovascular thrombotic events. It was proposed that the weaker COX-2 specificity of celecoxib compared to rofecoxib and valdecoxib (COX-1/COX-2 ratios of IC_{50} index of celecoxib, rofecoxib and valdecoxib are 37, 141 and 270, respectively) is responsible for the relative safety of celecoxib in relation to cardiovascular thrombotic events.[40–42] From this point of view, **31** may be safer for use with respect to possible cardiovascular thrombotic events compared to rofecoxib and valdecoxib.

4. Conclusion

We have found that a loxoprofen derivative, **31**, administered orally to rats, produced fewer gastric lesions but provided similar anti-inflammatory effects compared to **1**. This may be due to its selectivity for COX-2, resulting in a lower propensity for the gastric level of PGE_2 to be reduced. Although **31** exhibits higher membrane permeabilization activity and does not maintain the pro-drug characteristic of **1**, we consider that it is likely to be therapeutically beneficial as a safer NSAID.

5. Experimental

5.1. Molecular modeling studies

Docking studies were performed with MOE (The Molecular Operating Environment) Version 2009.10 software (Chemical Computing Group Inc., Montreal, Canada).

Table 2
In vitro membrane permeabilization assay and human whole blood assay for inhibition of COX-1- and COX-2-derived PG biosynthesis: loxoprofen derivatives with modification at the 3-position (**16–23**) and the 2-position (**24–31**) of the phenyl ring by a para-substituted aryl group

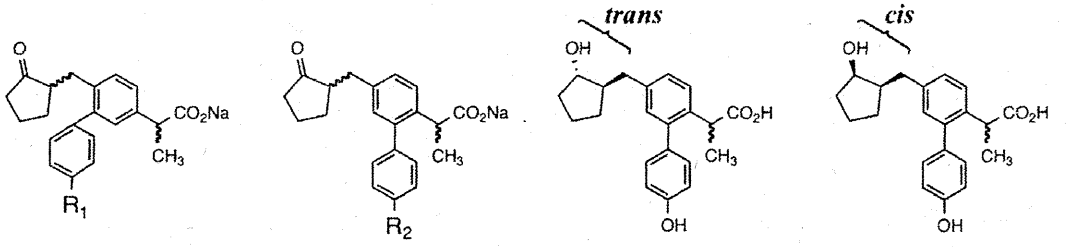

32 **33**

Compounds	R_1 or R_2	EC_{50} (mM)	IC_{50} (μM)		COX-1/COX-2
		Calcein release	COX-1	COX-2	
1		800[a]	24[a]	10[a]	2.5[a]
2			1.3[a]	2.4[a]	0.6[a]
3			6.3[a]	12.2[a]	0.6
16	$R_1 = H$	<100	54	290	0.2
17	$R_1 = CH_3$	<100	56	420	0.1
18	$R_1 = OCH_3$	<100	800	>1000	–
19	$R_1 = SCH_3$	<10	758	>1000	–
20	$R_1 = F$	<100	174	36	1.0
21	$R_1 = OCF_3$	<10	460	72	6.4
22	$R_1 = CO_2Na$	200	>1000	>1000	–
23	$R_1 = OH$	>1000	>1000	–	–
24	$R_2 = H$	<100	310	70	4.4
25	$R_2 = CH_3$	<100	470	540	0.9
26	$R_2 = OCH_3$	<100	74	430	0.2
27	$R_2 = SCH_3$	<100	575	150	3.8
28	$R_2 = F$	20	174	36	4.8
29	$R_2 = OCF_3$	6	515	>1000	–
30	$R_2 = CO_2Na$	<10	>1000	76	–
31	$R_2 = OH$	25	326	11	31
32			650	20	33
33			47	17	2.8
Celecoxib		0.09[a]	7[b]	0.19[b]	37[b]

Experiments and data analysis were performed as described in the legend of Table 1.
[a] Data from our previous report.[25]
[b] Data from a reference.[41]

5.1.1. Construction of the ligand molecule

The ligand molecule of (*S*)-2-{4-[((1*R*,2*S*)-2-hydroxycyclopentyl)methyl]phenyl}propanoic acid was constructed using the Builder module. The geometric stereochemistry was constrained, and all carboxylic acid groups were modeled in their ionized forms.

5.1.2. Construction of the receptor protein

The crystal structures of sheep COX-1 complexed with aspirin (1PTH)[30] and murine COX-2 complexed with indomethacin (4COX)[28] were obtained from the Protein Data Bank. After removal of the ligand and water, the structure of each receptor protein was optimized with the addition of hydrogen atoms and charge to acidic amino acid residues.

5.1.3. Molecular docking of the ligand with COX-1 and COX-2

Modeling calculations were performed only for each active site of COX-1 and COX-2 using the automatic docking program (ASE Dock 2005), which includes energy minimization applied to the ligand. The ligand–receptor complexes were subjected to energy minimization to convergence using the standard conditions at MMFF94 force fields. All amino acid residues within a 4.5 Å radius around the ligand were minimized, and the best conformation of ligand corresponding to the minimum docking energy of each ligand–receptor complex was adopted.

5.2. Chemistry

All solvents and reagents were purchased from Tokyo Kasei Chemical Co. (Tokyo, Japan) and Wako Pure Chemical Industries (Tokyo, Japan), and used without further purification. Fourier transform IR spectra were recorded on a JASCO FT/IR-410 spectrophotometer using potassium bromide (KBr) pellets. ^1H NMR and ^{13}C NMR spectra were recorded on a JNM AL-300 spectrometer (JEOL Ltd., Tokyo, Japan) operating at 300 MHz, in a ca. 2% solution of $CDCl_3$ or CD_3OD. Coupling constant (*J*) values are estimated in hertz (Hz) and spin multiples are given as s (singlet), d (doublet), t (triplet), q (quartet), m (multiplet), and br (broad). Mass spectra were detected with a fast atom bombardment (FAB) mass spectrometer (JMS-700, JEOL Ltd, Tokyo, Japan). The progress of all reactions was monitored by thin-layer chromatography (TLC) with silica gel glass plates (60 F_{254}) (Merck Ltd, Tokyo, Japan), and spots were visualized with ultraviolet (UV) light (254 nm) and stained in 5% ethanolic phosphomolybdic acid. Column chromatography was performed using Silica Gel 60 N (Kanto Chemical Co., Tokyo, Japan). Elemental analysis was performed for C and H (Instrumental Analysis Center, Kumamoto University) and was within ±0.4% of the theoretical values. Loxoprofen sodium (**1**), loxoprofen-OH (**2**, **3**), and compound **4b** were synthesized as reported previously.[25]

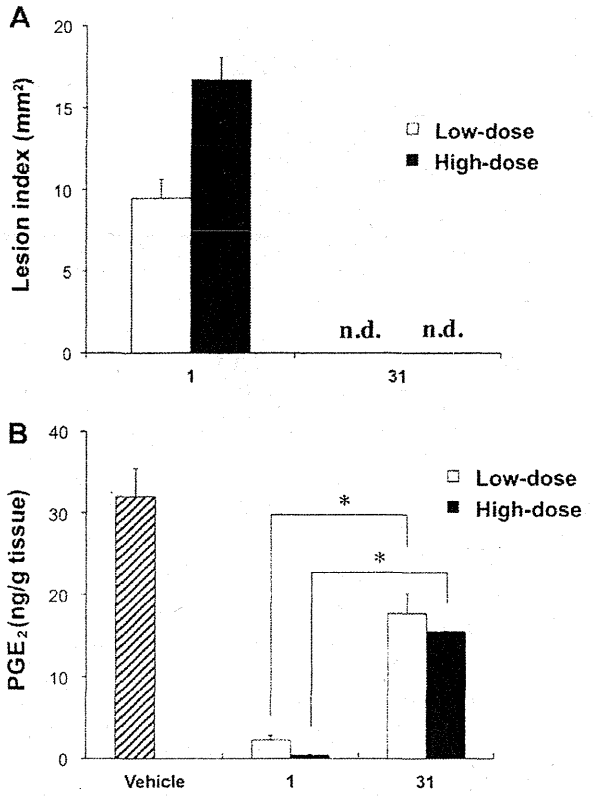

Figure 3. Production of gastric lesions and gastric PGE_2 levels in the presence of loxoprofen sodium and its derivative. Rats were orally administered a low (40 or 54 mg/kg) or high (50 or 67 mg/kg) dose of **1** or **31**, respectively, or vehicle and their stomachs were removed after 8 h. Stomachs were scored for hemorrhagic damage (A). Gastric PGE_2 level was determined by EIA (B). Values are mean ± SEM (n = 3–6). * P <0.05; n.d., not detected.

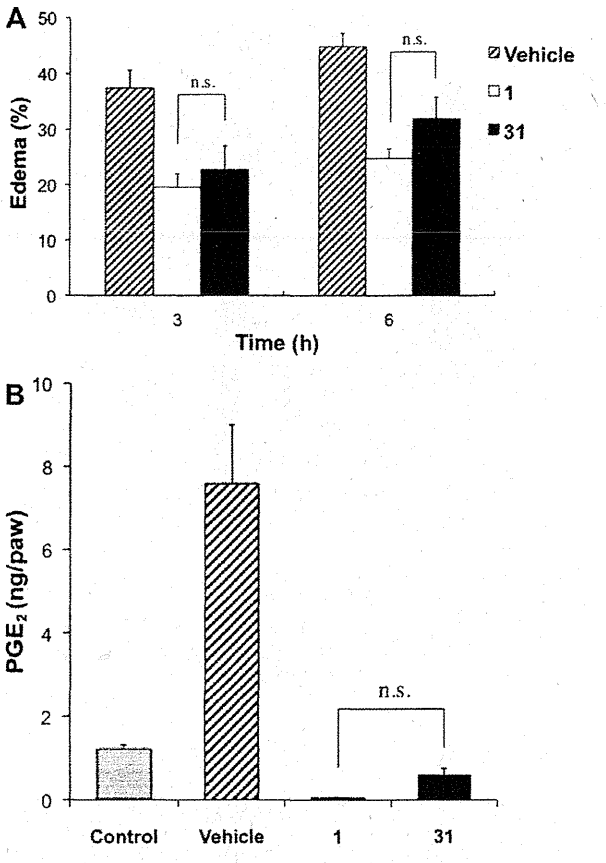

Figure 4. Anti-inflammatory activities of loxoprofen sodium and its derivative. Rats were orally administered 10 or 13 mg/kg of **1** or **31**, respectively, or vehicle and 1 h later received an intradermal injection of carrageenan (1%) into the left hindpaw. Footpad edema was measured 3 h and 6 h after the administration of carrageenan (A). The level of PGE_2 in the footpad was determined by EIA. Control rats were not treated with carrageenan (B). Values are mean ± SEM (n = 3–6). n.s., not significant.

5.2.1. Synthesis of 2-{2-halogeno (or nitro)-4-[(2-oxocyclopentyl)methyl]phenyl}propanoic acid (10a–c)

Compounds **10a–c** were synthesized from the corresponding starting materials **5a–c** by the method described previously.[25]

5.2.1.1. 2-Chloro-4-methylbenzaldehyde (6a). Yellow liquid (yield 52.0%), ^{1}H NMR ($CDCl_3$) δ: 2.34 (3H, s, Ar-CH_3), 7.66 (1H, d, J = 7.5, Ar-H5), 8.14 (1H, d, J = 7.5 Hz, Ar-H6), 8.90 (1H, s, Ar-H3), 10.34 (1H, br s, CHO). EI-MS (m/z): 154.07 (M^+).

5.2.1.2. 2-Iodo-4-methylbenzaldehyde (6b). Red-brown solid (yield 40.1%), ^{1}H NMR ($CDCl_3$) δ: 2.35 (3H, s, Ar-CH_3), 7.26 (1H, d, J = 8.1, Ar-H5), 7.89 (1H, d, J = 8.1 Hz, Ar-H6), 7.90 (1H, s, Ar-H3), 10.34 (1H, br s, CHO). EI-MS (m/z): 245.99 (M^+).

5.2.1.3. 4-Methyl-2-nitrobenzaldehyde (6c). Yellow liquid (yield 36.3%), ^{1}H NMR ($CDCl_3$) δ: 2.54 (3H, s, Ar-CH_3), 7.59 (1H, d, J = 8.4 Hz, Ar-H5), 7.87 (1H, d, J = 7.7 Hz, Ar-H6), 7.89 (1H, s, Ar-H3), 10.36 (1H, s, CHO). EI-MS (m/z): 164.99 (M^+).

5.2.1.4. 2-Chloro-4-methylphenylacetic acid (7a). White solid (yield 59.9%), ^{1}H NMR ($CDCl_3$) δ: 2.34 (3H, s, Ar-CH_3), 3.56 (2H, s, CH_2), 7.06 (1H, dd, J = 7.7, 1.8 Hz, Ar-H5), 7.17 (1H, d, J = 7.7 Hz, Ar-H6), 7.27 (1H, s, Ar-H3), 10.54 (1H, s, CO_2H). FAB-MS (m/z): 184.59 (M^+).

5.2.1.5. 2-Iodo-4-methylphenylacetic acid (7b). White solid (yield 61.3%), ^{1}H NMR ($CDCl_3$) δ: 2.29 (3H, s, Ar-CH_3), 3.76 (2H, s, CH_2), 7.21–7.70 (2H, m, Ar-H5, Ar-H6), 7.68 (1H, s, Ar-H3), 10.56 (1H, s, CO_2H). FAB-MS (m/z): 275.69 (M^+).

5.2.1.6. 4-Methyl-2-nitrophenylacetic acid (7c). White solid (yield 60.0%), ^{1}H NMR ($CDCl_3$) δ: 2.44 (3H, s, Ar-CH_3), 4.01 (2H, s, CH_2), 7.23 (1H, d, J = 7.7 Hz, Ar-H5), 7.41 (1H, d, J = 8.1 Hz), 7.95 (1H, s, Ar-H3), 10.66 (1H, s, CO_2H). FAB-MS (m/z): 196.21 (M^++H).

5.2.1.7. Methyl 2-(2-chloro-4-methylphenyl)propanoate (8a). Slightly-yellow liquid (yield: 71.4%), ^{1}H NMR ($CDCl_3$) δ: 1.48 (3H, d, J = 7.0 Hz, α-CH_3), 2.34 (3H, s, Ar-CH_3), 3.66 (3H, s, OCH_3), 3.66 (1H, q, J = 7.2 Hz, CH), 7.08 (1H, dd, J = 8.1, 1.8 Hz, Ar-H5), 7.17 (1H, d, J = 7.7 Hz, Ar-H6), 7.28 (1H, d, J = 1.8 Hz, Ar-H3). FAB-MS (m/z): 213.20 (M^++H).

5.2.1.8. Methyl 2-(2-iodo-4-methylphenyl)propanoate (8b). Colorless liquid (yield: 65.3%), ^{1}H NMR ($CDCl_3$) ^{1}H NMR ($CDCl_3$) δ: 1.44 (3H, d, J = 7.0 Hz, α-CH_3), 2.27 (3H, s, Ar-CH_3), 3.67 (3H, s, OCH_3), 4.07 (1H, q, J = 7.2 Hz, CH), 7.20–7.13 (2H, m, Ar-H5, Ar-H6), 7.69 (1H, s, Ar-H3). FAB-MS (m/z): 305.13 (M^++H).

5.2.1.9. Methyl 2-(4-methyl-2-nitrophenyl)propanoate (8c). Yellow liquid (yield: 54.3%), ^{1}H NMR ($CDCl_3$) δ: 1.58 (3H, d, J = 7.0 Hz, α-CH_3), 2.42 (3H, s, Ar-CH_3), 3.66 (3H, s, OCH_3), 4.27 (1H, q, J = 7.1 Hz, CH), 7.36–7.39 (2H, m, Ar-H5, Ar-H6), 7.74 (1H, s, Ar-H3). FAB-MS (m/z): 224.28 (M^++H).

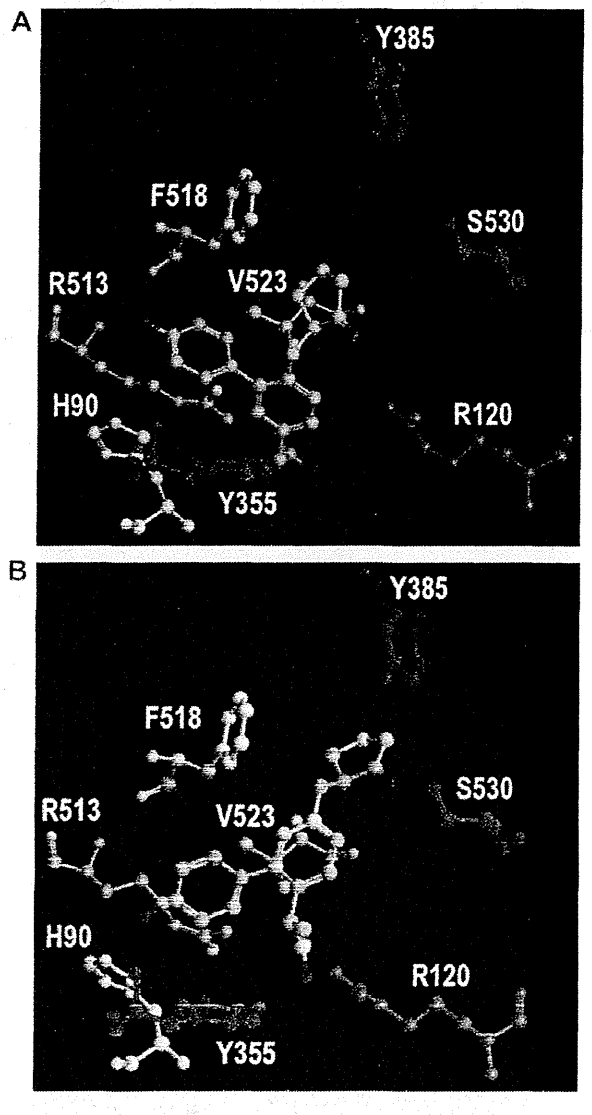

Figure 5. Potential binding mode of **23** (A) or **31** (B) to the active site of murine COX-2. Hydrogen atoms of the amino acid residues and the ligand have been removed.

5.2.1.10. Methyl 1-[3-chloro-4-(1-methoxy-1-oxopropan-2-yl)-benzyl]-2-oxocyclopentanecarboxylate (9a). Colorless liquid (yield: 54.0%), ^{1}H NMR (CD_3Cl_3) δ: 1.47 (3H, d, J = 7.3 Hz, α-CH_3), 1.69–2.14 (4H, m, H3′, H4′), 2.35–2.50 (2H, m, H5′), 3.22 (1H, d, J = 14.3 Hz, CH_2), 3.49 (1H, d, J = 14.3 Hz, CH_2), 3.66 (1H, q, J = 7.1 Hz, CH), 3.67 (3H, s, CO_2CH_3), 3.74 (3H, s, CO_2CH_3), 7.08 (1H, d, J = 8.1 Hz, Ar-H5), 7.14 (1H, d, J = 8.1 Hz, Ar-H6), 7.30 (1H, s, Ar-H3). FAB-MS (m/z): 353.21 (M^++H).

5.2.1.11. Methyl 1-[3-iodo-4-(1-methoxy-1-oxopropan-2-yl)-benzyl]-2-oxocyclopentanecarboxylate (9b). Colorless liquid (yield: 53.3%), ^{1}H NMR (CD_3Cl_3) δ: 1.43 (3H, d, J = 7.3 Hz, α-CH_3), 1.70–2.17 (4H, m, H3′, H4′), 2.36–2.47 (2H, m, H5′), 2.95 (1H, d, J = 13.9 Hz, CH_2), 3.17 (1H, d, J = 13.9 Hz, CH_2), 3.68 (3H, s, CO_2CH_3), 3.73 (3H, s, CO_2CH_3), 4.06 (1H, q, J = 7.1 Hz, CH), 7.10 (1H, d, J = 8.8 Hz, Ar-H5), 7.17 (1H, d, J = 8.1 Hz, Ar-H6), 7.64 (1H, s, Ar-H3). FAB-MS (m/z): 445.11 (M^++H).

5.2.1.12. Methyl 1-[4-(1-methoxy-1-oxopropan-2-yl)-3-nitrobenzyl]-2-oxocyclopentanecarboxylate (9c). Yellow liquid (yield: 38.6%), ^{1}H NMR (CD_3Cl_3) δ: 1.58 (3H, d, J = 7.3 Hz, α-CH_3), 1.75–2.22 (4H, m, H3′, H4′), 2.40–2.51 (2H, m, H5′), 3.05 (1H, d, J = 14.1 Hz, CH_2), 3.32 (1H, d, J = 13.9 Hz, CH_2), 3.67 (3H, s, CO_2CH_3), 3.74 (3H, s, CO_2CH_3), 4.28 (1H, q, J = 7.2 Hz, CH), 7.39 (2H, br s, Ar-H5, Ar-H6), 7.73 (1H, br s, Ar-H3). FAB-MS (m/z): 364.31 (M^++H).

5.2.1.13. Sodium 2-{2-chloro-4-[(2-oxocyclopentyl)methyl]-phenyl}propanoate (10a). White solid (yield: 96.0%), IR (KBr) ν: 1736 (CO_2^-), 1713 (C=O), cm^{-1}. ^{1}H NMR (CD_3OD) δ: 1.38 (3H, d, J = 7.1 Hz, α-CH_3), 1.53–2.03 (4H, m, H3′, H4′), 2.06–2.58 (4H, m, H1′, H5′, CH_2), 3.23 (1H, dd, J = 12.7, 3.2 Hz, CH_2), 3.52 (1H, q, J = 7.1 Hz, CH), 7.15 (1H, d, J = 7.9 Hz, Ar-H5), 7.21 (1H, d, J = 7.9 Hz, Ar-H6), 7.38 (1H, s, Ar-H3). ^{13}C NMR (CD_3OD) δ: 19.80 (α-CH_3), 21.44 (C5′), 30.17 (C4′), 33.69 (CH_2), 38.80 (C3′), 49.68 (CH), 50.71 (C1′), 127.43 (Ar-C5), 129.53 (Ar-C3), 131.81 (Ar-C1), 134.56 (Ar-C6), 136.34 (Ar-C2), 145.69 (Ar-C4), 182.40 (CO_2Na), 222.45 (C=O). HR-FAB-MS (m/z): 325.0580 (M^++Na, calcd for $C_{15}H_{16}ClNa_2O_3$: 325.0583). Anal. Calcd for $C_{15}H_{16}ClNa_2O_3 \cdot H_2O$: C, 56.17; H, 5.66. Found: C, 56.25, H, 5.75.

5.2.1.14. Sodium 2-{2-iodo-4-[(2-oxocyclopentyl)methyl]phenyl}propanoate (10b). White solid (yield: 94.1%), IR (KBr) ν: 1733 (CO_2^-), 1715 (C=O), cm^{-1}. ^{1}H NMR (CD_3OD) δ: 1.34 (3H, d, J = 7.0 Hz, α-CH_3), 1.48–2.14 (4H, m, H3′, H4′), 2.01–2.38 (3H, m, H1′, H5′), 2.46 (1H, dd, J = 13.4, 9.0 Hz, CH_2), 2.98 (1H, dd, J = 13.0, 3.5 Hz, CH_2), 3.85 (1H, q, J = 7.1 Hz, CH), 7.12 (1H, d, J = 8.1 Hz, Ar-H5), 7.34 (1H, d, J = 8.1 Hz, Ar-H6), 7.64 (1H, s, Ar-H3). ^{13}C NMR (CD_3OD) δ: 20.04 (α-CH_3), 21.42 (C5′), 29.97 (C4′), 35.27 (CH_2), 38.95 (C3′), 51.93 (CH), 54.07 (C1′), 102.35 (Ar-C2), 128.70 (Ar-C5), 130.13 (Ar-C6), 140.61 (Ar-C4), 141.10 (Ar-C3), 146.39 (Ar-C1), 182.03 (CO_2Na), 222.54 (C=O). HR-FAB-MS (m/z): 416.9935 (M^++Na, calcd for $C_{15}H_{16}INa_2O_3$: 416.9940). Anal. Calcd for $C_{21}H_{21}NaO_3 \cdot H_2O$: C, 43.71; H, 4.40. Found: C, 43.64, H, 4.22.

5.2.1.15. Sodium 2-{2-nitro-4-[(2-oxocyclopentyl)methyl]phenyl}propanoate (10c). Yellow solid (yield: 69.4%), IR (KBr) ν: 1738 (CO_2^-), 1711 (C=O), cm^{-1}. ^{1}H NMR (CD_3OD) δ: 1.39 (3H, d, J = 7.3 Hz, α-CH_3), 1.53–2.07 (4H, m, H3′, H4′), 1.94–2.38 (3H, m, H1′, H5′), 2.52 (1H, dd, J = 7.1, 3.5 Hz, CH_2), 3.02 (1H, dd, J = 13.9, 5.1 Hz, CH_2), 3.92 (1H, q, J = 7.1 Hz, CH), 7.32 (1H, d, J = 8.1 Hz, Ar-H5), 7.45 (1H, d, J = 8.1 Hz, Ar-H6), 7.55 (1H, s, Ar-H3). ^{13}C NMR (CD_3OD) δ: 19.82 (α-CH_3), 21.21 (C5′), 29.85 (C4′), 35.38 (CH_2), 38.86 (C3′), 45.17 (CH), 51.71 (C1′), 125.18 (Ar-C3), 130.85 (Ar-C1), 134.31 (Ar-C6), 137.74 (Ar-C5), 140.78 (Ar-C4), 151.04 (Ar-C2), 181.20 (CO_2Na), 222.26 (C=O). HR-FAB-MS (m/z): 336.0814 (M^++Na, calcd for $C_{15}H_{16}NNa_2O_5$: 336.0824). Anal. Calcd for $C_{15}H_{16}NNaO_5 \cdot H_2O$: C, 54.38; H, 5.48; N, 4.23. Found: C, 54.36, H, 5.45, N, 4.09.

5.2.2. Synthesis of loxoprofen derivatives with modification at the 3-position of the phenyl ring (15–23)

5.2.2.1. Methyl 2-(3-bromophenyl)propanoate (12). (3-Bromophenyl)acetic acid **11** (5.0 g, 23.3 mmol) and methanol (50 mL) were refluxed for 3 h in the presence of 0.2 mL of concentrated hydrochloric acid (HCl) to give the methyl (3-bromophenyl)acetate. After neutralization with saturated $NaHCO_3$ and washing with brine, a pure product was obtained from the diethyl ether extract. This methyl acetate (4.9 g, 21.4 mmol) in dry THF (35 mL) was added dropwise to a stirred solution of 2.0 mol/L lithium diisopropylamide (LDA) (12.9 mL, 25.8 mmol) in THF/ethylbenzene/heptane at −78 °C under argon (Ar), and after 30 min, iodomethane (CH_3I) (2.0 mL, 32.2 mmol) was added slowly. The resulting solution was stirred for 5 h with the temperature changed from −78 to −40 °C, then evaporated to dryness, and extracted with CH_2Cl_2 (50 mL). Evaporation of the solvent and purification of the residue

by silica gel chromatography (*n*-hexane/AcOEt, 20:1) yielded the title compound as a colorless liquid (77.2%). ^{1}H NMR ($CDCl_3$) δ: 1.49 (3H, d, J = 7.1 Hz, α-CH_3), 3.67 (3H, s, CO_2CH_3), 3.68 (1H, q, J = 7.1 Hz, CH), 7.18 (1H, t, J = 7.5 Hz, Ar-H5), 7.23 (1H, dt, J = 7.8, 1.7 Hz, Ar-H6), 7.38 (1H, dt, J = 7.3, 1.8 Hz, Ar-H4), 7.44 (1H, st, J = 1.7 Hz, Ar-H2). FAB-MS (*m/z*): 243.02 (M^++H, calcd for $C_{10}H_{12}{}^{79}BrO_2$: 243.00).

5.2.2.2. Methyl 2-[3-bromo-4-(chloromethyl)phenyl]propanoate (13). To a suspension of aluminium(III) chloride ($AlCl_3$) (1.52 g, 11.4 mmol) in CH_2Cl_2 (10 mL), 1,3-dioxolane (1.21 mL, 17.5 mmol) was added and the mixture was stirred at 0 °C for 30 min. Tin (IV) chloride ($SnCl_4$) (2.68 mL, 14.6 mmol), **5** (1.78 g, 7.31 mmol) in CH_2Cl_2 (5 mL) and chloromethylmethyl ether (5.50 mL, 73.1 mmol) were added to the reaction mixture. After stirring at room temperature for 20 h, the mixture was poured into dilute HCl solution, and the product was extracted with CH_2Cl_2. Evaporation of the solvent and purification of the residue by silica gel chromatography (*n*-hexane/AcOEt, 10:1) yielded the title compound as a colorless liquid (50.3%). ^{1}H NMR ($CDCl_3$) δ: 1.49 (3H, d, J = 7.3 Hz, α-CH_3), 3.67 (3H, s, CO_2CH_3), 3.70 (1H, q, J = 7.1 Hz, CH), 4.67 (2H, s, CH_2), 7.26 (1H, dd, J = 7.9, 1.8 Hz, Ar-H6), 7.43 (1H, d, J = 7.9 Hz, Ar-H5), 7.53 (1H, sd, J = 1.8 Hz, Ar-H2). FAB-MS (*m/z*): 291.12 (M^++H, calcd for $C_{11}H_{13}{}^{79}BrClO_2$: 290.98).

5.2.2.3. Methyl 1-[2-bromo-4-(1-methoxy-1-oxopropan-2-yl)-benzyl]-2-oxocyclopentanecarboxylate (14). To a suspension of potassium carbonate (K_2CO_3) (1.26 g, 9.1 mmol) in acetone (20 mL), methyl 2-oxocyclopentanecarboxylate (0.64 mL, 5.1 mmol) was added and the mixture was stirred at room temperature for 30 min. A solution of **13** (1.47 g, 5.1 mmol) in acetone (5 mL) was added and the resulting mixture was refluxed for 12 h. The reaction mixture was cooled to room temperature, filtered through paper, and the filtrate was evaporated to dryness. The resulting residue was purified on silica gel chromatography (*n*-hexane/AcOEt, 7:2) to yield the title compound as a colorless oil (78.0%). ^{1}H NMR (CD_3Cl_3) δ: 1.47 (3H, d, J = 7.3 Hz, α-CH_3), 1.71–2.13 (4H, m, H3′, H4′), 2.36–2.55 (2H, m, H5′), 3.28 (1H, d, J = 14.3 Hz, CH_2), 3.51 (1H, d, J = 14.3 Hz, CH_2), 3.66 (1H, q, J = 7.3 Hz, CH), 3.67 (3H, s, CO_2CH_3), 3.74 (3H, s, CO_2CH_3), 7.12 (2H, d, J = 0.7 Hz, Ar-H5, Ar-H6), 7.49 (1H, s, Ar-H2). FAB-MS (*m/z*): 396.22 (M^++H, calcd for $C_{18}H_{21}{}^{79}BrO_5$: 396.06).

5.2.2.4. General procedure for the decarboxylation and hydrolysis by acid. To the bis-methylester intermediate **14** (ca. 5 mmol) in acetic acid (AcOH) (40 mL), concentrated HCl (80 mL) was added and the mixture was refluxed for 12 h. After cooling to room temperature, the reaction mixture was evaporated to dryness. The resulting residue was diluted with CH_2Cl_2 (50 mL), followed by addition of saturated NaHCO3 solution (50 mL). After removal of organic layer, CH_2Cl_2 (30 mL) was added, and the aqueous layer was adjusted to acidity (pH 1) with 6 M HCl. The organic layer was extracted with CH_2Cl_2, dried over anhydrous Na_2SO_4, and evaporated to dryness. The resulting precipitate was collected to yield the carboxylic acid (precursor of **15**) (92%).

5.2.2.5. General procedure for preparation of the sodium salts of compounds. To a solution of the carboxylic acid (precursor of **15**) in EtOH (30 mL), 1 M NaOH solution (1.0 equiv, ca. 2.2 mmol) was added and refluxed for 2 h. After cooling to room temperature, the resulting mixture was evaporated to dryness. The precipitated product was collected, and recrystallized with ethanol/ether to yield title compounds **15**.

*5.2.2.5.1. Sodium 2-{3-bromo-4-[(2-oxocyclopentyl)methyl]phenyl}propanoate (**15**).* ^{1}H NMR (CD_3OD) δ: 1.38 (3H, d, J = 7.3 Hz, α-CH_3), 1.53–2.02 (4H, m, H3′, H4′), 2.07–2.50 (3H, m, H1′, H5′), 2.56 (1H, dd, J = 13.9, 9.3 Hz, CH_2), 3.22 (1H, dd, J = 13.6, 4.8 Hz, CH_2), 3.52 (1H, q, J = 7.2 Hz, CH), 7.15 (1H, d, J = 7.7 Hz, Ar-H5), 7.26 (1H, d, J = 7.7 Hz, Ar-H6), 7.56 (1H, s, Ar-H3). ^{13}C NMR (CD_3OD) δ: 19.83 (α-CH_3), 21.44 (C5′), 30.15 (C4′), 36.19 (CH_2), 38.80 (C3′), 49.62 (CH), 50.75 (C1′), 125.00 (Ar-C3), 128.04 (Ar-C6), 131.78 (Ar-C5), 132.88 (Ar-C2), 138.05 (Ar-C1), 145.91 (Ar-C4), 182.38 (CO_2Na), 222.37 (C=O). HR-FAB-MS (*m/z*): 369.0089 (M^++Na, *calcd for* $C_{15}H_{16}{}^{79}BrNa_2O_3$: 369.0078). Anal. Calcd for $C_{15}H_{16}{}^{79}BrNaO_3{\cdot}H_2O$: C, 49.33; H, 4.97. Found: C, 49.42, H, 5.05.

5.2.2.6. General procedure for the Suzuki–Miyaura cross-coupling reaction. The intermediate **14** (1.0 equiv, ca. 0.9 mmol) and each arylboronic acid (R-PhB(OH)$_2$) (1.5 equiv) were dissolved in THF (16 mL), followed by addition of 2 M Na_2CO_3 in water (3 mL) and $Pd(PPh_3)_4$ (0.03 equiv). After refluxing overnight, the reaction mixture was cooled to room temperature, and diluted with water. The mixture was extracted with AcOEt, dried over anhydrous sodium sulfate (Na_2SO_4), and filtered. The filtrate was evaporated to dryness, and the residue was purified on silica gel chromatography (*n*-hexane/AcOEt, 7:2) to yield the biphenyl compound (bis-methylester intermediate, the precursor of **16–23**) as a yellow oil (52–85%). Decarboxylation, hydrolysis by acid and sodium salt preparation of the bis-methylester intermediate (the precursor of **16–23**) was done as described above to yield **16–23**.

*5.2.2.6.1. Sodium 2-{6-[(2-oxocyclopentyl)methyl]biphenyl-3-yl}-propanoate (**16**).* Yield: 69%, three steps. IR (KBr) ν: 1423, 1712 (CO_2^-), 1730 (C=O), cm^{-1}. ^{1}H NMR (CD_3OD) δ: 1.32 (3H, d, J = 7.3 Hz, α-CH_3), 1.42–2.35 (6H, m, H3′, H4′, H5′), 2.38–2.50 (1H, m, H1′), 3.05 (1H, dd, J = 14.1, 3.0 Hz, CH_2), 3.14 (1H, d, J = 12.4, 3.0 Hz, CH_2), 3.48 (1H, q, J = 7.1 Hz, CH), 7.05–7.10 (3H, s, Ar-H5, Ar-H6), 7.23 (3H, m, Ar-H2′, Ar-H4′), 7.25–7.31 (2H, m, Ar-H3′), 7.47 (1H, s, Ar-H2). ^{13}C NMR (CD_3OD) δ: 19.88 (α-CH_3), 21.39 (C5′), 30.23 (C4′), 33.32 (CH_2), 36.20 (C3′), 38.79 (CH), 51.65 (C1′), 127.80 (Ar-C5), 128.07 (Ar-C4′), 129.13 (Ar-C2′), 130.44 (Ar-C6), 130.48 (Ar-C3′), 131.78 (Ar-C2), 132.93 (Ar-C1, Ar-C3), 136.08 (Ar-C4), 138.05 (Ar-C4), 143.52 (Ar-C1′), 183.38 (CO_2Na), 222.83 (C=O). HR-FAB-MS (*m/z*): 367.1289 (M^++Na, calcd for $C_{21}H_{21}Na_2O_3$: 367.1286). Anal. Calcd for $C_{21}H_{21}NaO_3{\cdot}H_2O$: C, 76.11; H, 7.00. Found: C, 76.24, H, 7.05.

*5.2.2.6.2. Sodium 2-{4′-methyl-6-[(2-oxocyclopentyl)methyl]biphenyl-3-yl}propanoate (**17**).* Yield: 70%, three steps. IR (KBr) ν: 1420, 1711 (CO_2^-), 1733 (C=O), cm^{-1}. ^{1}H NMR (CD_3OD) δ: 1.30–2.16 (6H, m, H3′, H4′, H5′), 1.41 (3H, d, J = 7.3 Hz, α-CH_3), 2.31 (3H, s, Ar-CH_3), 2.34–2.24 (1H, m, H1′), 2.48 (1H, dd, J = 20.5, 12.8 Hz, CH_2), 3.16 (1H, dd, J = 24.4, 13.7 Hz, CH_2), 3.64 (1H, q, J = 7.1 Hz, CH), 7.10 (1H, d, Ar-H6), 7.16–7.18 (5H, m, Ar-H5, Ar-H2′, Ar-H3′), 7.49 (1H, s, Ar-H2). ^{13}C NMR (CD_3OD) δ: 19.22 (α-CH_3), 21.33 (C5′), 30.14 (C4′), 33.30 (Ar-CH_3), 36.32 (CH_2), 38.82 (C3′), 45.79 (CH), 50.40 (C1′), 125.23 (Ar-C5), 127.84 (Ar-C6), 129.84 (Ar-C2′), 130.15 (Ar-C3′), 132.18 (Ar-C3), 132.81 (Ar-C4′), 137.42 (Ar-C2), 140.08 (Ar-C4), 142.54 (Ar-C1), 143.55 (Ar-C1′), 178.38 (CO_2Na), 222.18 (C=O). HR-FAB-MS (*m/z*): 381.1447 (M^++Na, calcd for $C_{22}H_{23}Na_2O_3$: 381.1443). Anal. Calcd for $C_{22}H_{23}NaO_3{\cdot}H_2O$: C, 76.11; H, 7.00. Found: C, 76.24, H, 7.05.

*5.2.2.6.3. Sodium 2-{4′-methoxy-6-[(2-oxocyclopentyl)methyl]-biphenyl-3-yl}propanoate (**18**).* Yield: 75%, three steps. IR (KBr) ν: 1416, 1713 (CO_2^-), 1729 (C=O), cm^{-1}. ^{1}H NMR (CD_3OD) δ: 1.21–2.04 (6H, m, H3′, H4′, H5′), 1.41 (3H, d, J = 7.0 Hz, α-CH_3), 2.07–2.22 (1H, m, H1′), 2.39 (1H, dd, J = 14.5, 3.1 Hz, CH_2), 3.15 (1H, dd, J = 14.1, 5.3 Hz, CH_2), 3.57 (1H, q, J = 7.1 Hz, CH), 2.80 (3H, s, Ar-OCH_3), 6.93 (2H, d, J = 7.1 Hz, Ar-H3′), 7.15 (1H, d, J = 7.7 Hz, Ar-H6), 7.17 (1H, s, Ar-H2), 7.19 (2H, d, J = 6.2 Hz, Ar-H2′), 7.27 (1H, dd, J = 8.1, 1.8 Hz, Ar-H5). ^{13}C NMR (CD_3OD) δ: 18.96 (α-CH_3), 21.46 (C5′), 30.27 (C4′), 33.69 (CH_2), 38.56 (C3′), 46.19 (CH), 51.45 (C1′), 55.79 (Ar-OCH_3), 114.85 (Ar-C3′), 115.44 (Ar-C5), 127.34 (Ar-C6), 130.53 (Ar-C2′), 131.37 (Ar-C1′), 137.68

(Ar-C2), 140.20 (Ar-C1), 143.44 (Ar-C3), 157.64 (Ar-C4), 160.28 (Ar-C4′), 178.51 (CO_2Na), 222.83 (C=O). HR-FAB-MS (*m/z*): 397.1389 (M^++Na, calcd for $C_{22}H_{23}Na_2O_4$: 397.1392). Anal. Calcd for $C_{22}H_{23}NaO_4{\cdot}0.5H_2O$: C, 68.92; H, 6.31. Found: C, 68.88, H, 6.25.

*5.2.2.6.4. Sodium 2-{4′-(methylthio)-6-[(2-oxocyclopentyl)met]-hylbiphenyl-3-yl}propanoate (**19**).* Yield: 74%, three steps. IR (KBr) *ν*: 1417, 1711 (CO_2^-), 1731 (C=O), cm^{-1}. ^1H NMR (CD_3OD) *δ*: 1.24–2.22 (7H, m, H1′, H3′, H4′, H5′), 1.41 (3H, d, *J* = 7.0 Hz, α-CH_3), 2.40 (1H, dd, *J* = 13.9, 10.3 Hz, CH_2), 2.49 (3H, s, Ar-SCH_3), 3.15 (1H, dd, *J* = 13.9, 4.4 Hz, CH_2), 3.57 (1H, q, *J* = 7.1 Hz, CH), 7.15–7.23 (4H, m, Ar-H5, Ar-H6, Ar-H3′), 7.27–7.30 (3H, m, Ar-H2, Ar-H2′). ^{13}C NMR (CD_3OD) *δ*: 15.74 (Ar-SCH_3), 19.96 (α-CH_3), 21.31 (C5′), 30.33 (C4′), 33.37 (CH_2), 38.71 (C3′), 49.91 (CH), 51.66 (C1′), 127.32 (Ar-C3′), 127.78 (Ar-C5), 130.46 (Ar-C1), 130.54 (Ar-C6), 130.94 (Ar-C2′), 136.18 (Ar-C3), 138.58 (Ar-C2), 140.23 (Ar-C1′), 142.54 (Ar-C4), 143.41 (Ar-C4′), 183.03 (CO_2Na), 222.83 (C=O). HR-FAB-MS (*m/z*): 413.1169 (M^++Na, calcd for $C_{22}H_{23}Na_2SO_3$: 413.1163). Anal. Calcd for $C_{22}H_{23}NaSO_3{\cdot}0.5H_2O$: C, 66.15; H, 6.06. Found: C, 66.28, H, 6.05.

*5.2.2.6.5. Sodium 2-{4′-fluoro-6-[(2-oxocyclopentyl)methyl]biphenyl-3-yl}propanoate (**20**).* Yield: 68%, three steps. IR (KBr) *ν*: 1203 (Ar-F), 1410, 1709 (CO_2^-), 1730 (C=O), cm^{-1}. ^1H NMR (CD_3OD) *δ*: 1.23–2.23 (7H, m, H1′, H3′, H4′, H5′), 1.41 (3H, d, *J* = 7.3 Hz, α-CH_3), 2.39 (1H, dd, *J* = 14.1, 10.1 Hz, CH_2), 3.13 (1H, dd, *J* = 14.1, 4.2 Hz, CH_2), 3.58 (1H, q, *J* = 7.2 Hz, CH), 7.07–7.19 (4H, m, Ar-H5, Ar-H6, Ar-H3′), 7.25–7.31 (3H, m, Ar-H2, Ar-H2′). ^{13}C NMR (CD_3OD) *δ*: 19.95 (α-CH_3), 21.31 (C5′), 30.32 (C4′), 33.32 (CH_2), 38.68 (C3′), 49.91 (CH), 51.66 (C1′), 115.83 (d, J_{C-F} = 21.1 Hz, Ar-C3′), 127.97 (Ar-C5), 130.54 (d, J_{C-F} = 3.7 Hz, Ar-C2′), 132.19 (Ar-C6), 132.29 (Ar-C2), 132.29 (Ar-C1), 139.60 (d, J_{C-F} = 3.1 Hz, Ar-C1′), 142.06 (Ar-C3), 143.46 (Ar-C4), 164.98 (Ar-C4′), 183.02 (CO_2Na), 222.67 (C=O). HR-FAB-MS (*m/z*): 385.1199 (M^++Na, calcd for $C_{21}H_{20}FNa_2O_3$: 385.1192). Anal. Calcd for $C_{21}H_{20}FNaO_3{\cdot}H_2O$: C, 66.31; H, 5.83. Found: C, 66.28, H, 5.99.

*5.2.2.6.6. Sodium 2-{6-[(2-oxocyclopentyl)methyl]-4′-(trifluoromethoxy)biphenyl-3-yl}propanoate (**21**).* Yield: 54%, three steps. IR (KBr) *ν*: 1422, 1709 (CO_2^-), 1731 (C=O), cm^{-1}. ^1H NMR (CD_3OD) *δ*: 1.35–2.23 (7H, m, H1′, H3′, H4′, H5′), 1.41 (3H, d, *J* = 7.3 Hz, α-CH_3), 2.41 (1H, dd, *J* = 7.1, 3.5 Hz, CH_2), 3.14 (1H, dd, *J* = 14.1, 5.7 Hz, CH_2), 3.58 (1H, q, *J* = 7.1 Hz, CH), 7.19–7.40 (7H, m, Ar-H2, Ar-H5, Ar-H6, Ar-H2′, Ar-H3′). ^{13}C NMR (CD_3OD) *δ*: 19.95 (α-CH_3), 21.30 (C5′), 30.34 (C4′), 33.24 (CH_2), 38.66 (C3′), 49.91 (CH), 51.69 (C1′), 121.70 (d, *J* = 1.2 Hz, Ar-C3′), 128.24 (Ar-C5), 129.27 (Ar-OCF_3), 130.43 (Ar-C6), 130.61 (Ar-C1′), 132.19 (Ar-C2′), 136.16 (Ar-C2), 141.64 (Ar-C1), 142.63 (Ar-C3), 143.61 (Ar-C4), 149.48 (d, *J* = 1.2 Hz, Ar-C4′), 183.02 (CO_2Na), 222.57 (C=O). HR-FAB-MS (*m/z*): 451.1112 (M^++Na, calcd for $C_{22}H_{20}F_3Na_2O_4$: 451.1109). Anal. Calcd for $C_{22}H_{20}F_3NaO_4{\cdot}H_2O$: C, 59.19; H, 4.97. Found: C, 59.22, H, 5.00.

*5.2.2.6.7. Sodium 5′-(1-carboxylatoethyl)-2′-[(2-oxocyclopentyl)]-methyl]biphenyl-4-carboxylate (**22**).* Yield: 81%, three steps. IR (KBr) *ν*: 1424, 1690, 1720 (CO_2^-), 1728 (C=O), cm^{-1}. ^1H NMR (CD_3OD) *δ*: 1.18–2.17 (7H, m, H1′, H3′, H4′, H5′), 1.38 (3H, d, *J* = 7.1 Hz, α-CH_3), 2.38 (1H, dd, *J* = 14.5, 10.1 Hz, CH_2), 3.11 (1H, dd, *J* = 14.1, 5.1 Hz, CH_2), 3.55 (1H, q, *J* = 7.0 Hz, CH), 7.15–7.28 (5H, m, Ar-H2, Ar-H5, Ar-H6, Ar-H2′), 7.95 (2H, dd, *J* = 6.5, 1.9 Hz, Ar-H3′). ^{13}C NMR (CD_3OD) *δ*: 19.02 (α-CH_3), 21.30 (C5′), 30.39 (C4′), 33.32 (CH_2), 38.58 (C3′), 46.16 (CH), 51.61 (C1′), 128.17 (Ar-C5), 130.06 (Ar-C6), 130.59 (Ar-C2′), 130.62 (Ar-C3′), 130.75 (Ar-C2), 131.19 (Ar-C1), 137.46 (Ar-C3), 140.53 (Ar-C4), 142.70 (Ar-C4′), 147.85 (Ar-C1′), 169.66 (Ar-CO_2Na), 178.18 (CO_2Na), 222.35 (C=O). HR-FAB-MS (*m/z*): 433.1002 (M^++Na, calcd for $C_{22}H_{20}Na_3O_5$: 433.1004). Anal. Calcd for $C_{22}H_{20}Na_2O_5{\cdot}2H_2O$: C, 59.19; H, 5.42. Found: C, 59.31, H, 5.27.

*5.2.2.6.8. Sodium 2-{4′-hydroxy-6-[(2-oxocyclopentyl)methyl]]-biphenyl-3-yl}propanoate (**23**).* Yield: 47%, three steps. IR (KBr) *ν*: 1316 (Ar-OH), 1422, 1714 (CO_2^-), 1733 (C=O), cm^{-1}. ^1H NMR (CD_3OD) *δ*: 1.36–2.23 (7H, m, H1′, H3′, H4′, H5′), 1.40 (3H, d, *J* = 6.6 Hz, α-CH_3), 2.40 (1H, dd, *J* = 13.9, 10.3 Hz, CH_2), 3.15 (1H, dd, *J* = 13.9, 4.4 Hz, CH_2), 3.56 (1H, q, *J* = 6.8 Hz, CH), 6.80 (2H, dd, *J* = 6.6, 2.2 Hz, Ar-H3′), 7.17–7.07 (4H, m, Ar-H2, Ar-H6, Ar-H2′), 7.24 (1H, dd, *J* = 7.7, 1.8 Hz, Ar-H5). ^{13}C NMR (CD_3OD) *δ*: 19.97 (α-CH_3), 21.30 (C5′), 30.27 (C4′), 33.45 (CH_2), 38.77 (C3′), 50.00 (CH), 51.61 (C1′), 115.90 (Ar-C3′), 127.34 (Ar-C5), 130.43 (Ar-C6), 130.66 (Ar-C1′), 131.45 (Ar-C2′), 134.68 (Ar-C2), 136.29 (Ar-C1), 143.09 (Ar-C3), 143.28 (Ar-C4), 157.41 (Ar-C4′), 183.24 (CO_2Na), 223.09 (C=O). HR-FAB-MS (*m/z*): 360.1332 (M^++Na, calcd for $C_{21}H_{21}Na_2O_4$: 360.1338). Anal. Calcd for $C_{21}H_{21}NaO_4{\cdot}H_2O$: C, 66.66; H, 6.13. Found: C, 66.58, H, 6.11.

5.2.3. Synthesis of loxoprofen derivatives with modification at the 2-position of the phenyl ring by para-substituted aryl group (24–31)

A carboxy group of 2-{2-bromo-4-[(2-oxocyclopentyl)methyl]phenyl}propanoic acid was methyl esterificated to give methyl 2-{2-bromo-4-[(2-oxocyclopentyl)methyl]phenyl}propanoate (see below), which was then reacted with corresponding arylboronic acid under the conditions of Suzuki–Miyaura coupling reaction, as described above. The resulting biphenyl compounds were hydrolyzed by base (see below), and converted to the sodium salt by the same procedure described above.

5.2.3.1. Methyl ester protection of the carboxy group of 2-{2-bromo-4-[(2-oxocyclopentyl)methyl]phenyl}propanoic acid. To 2-{2-bromo-4-[(2-oxocyclopentyl)methyl]phenyl}propanoic acid (1.5 equiv, ca. 3.3 mmol) in CH_2Cl_2 (30 mL) and methanol (2 equiv, ca. 4.4 mmol), DMAP (1 equiv, ca. 2.2 mmol) and EDC (2 equiv, ca. 4.4 mmol) were added, followed by stirring for 15 min at room temperature. The reaction mixture was poured into cold water, and the resulting solution was extracted with CH_2Cl_2. Evaporation of the solvent and purification of the residue by silica gel chromatography (*n*-hexane/AcOEt, 3:1) yielded methyl 2-{2-bromo-4-[(2-oxocyclopentyl)methyl]phenyl}propanoate as a colorless oil (92%).

5.2.3.2. General procedure for alkaline hydrolysis. To the methylester intermediate (biphenyl compound from **4b**) (ca. 5 mmol) in ethanol (20 mL), 0.063 mM aqueous solution of KOH (5 mL) was added and refluxed for 2 h. After cooling to room temperature, the reaction mixture was evaporated to dryness. The resulting residue was diluted with CH_2Cl_2 (50 mL) and saturated $NaHCO_3$ solution (50 mL) was added. The organic layer was removed, CH_2Cl_2 (30 mL) was added, and the aqueous layer was adjusted to acidity (pH 1) with 6 M HCl. The organic layer was extracted with CH_2Cl_2, dried over anhydrous Na_2SO_4, and evaporated to dryness. The resulting precipitate was collected to yield the precursor of **24–31** (90–94%).

5.2.3.3. Sodium 2-{5-[(2-oxocyclopentyl)methyl]biphenyl-2-yl}propanoate (24). Yield: 74%, three steps. IR (KBr) *ν*: 1422, 1713 (CO_2^-), 1731 (C=O), cm^{-1}. ^1H NMR (CD_3OD) *δ*: 1.23 (3H, dd, *J* = 7.3, 1.5 Hz, α-CH_3), 1.56–2.44 (7H, m, H1′, H3′, H4′, H5′), 2.53 (1H, dd, *J* = 13.6, 9.2 Hz, CH_2), 3.05 (1H, d, *J* = 13.7, 4.2 Hz, CH_2), 3.71 (1H, q, *J* = 7.2 Hz, CH), 6.94 (1H, s, Ar-H3), 7.10 (1H, d, *J* = 8.1 Hz, Ar-H5), 7.32–7.39 (5H, m, Ar-H2′, Ar-H3′, Ar-H4′), 7.46 (1H, d, *J* = 8.1 Hz, Ar-H6). ^{13}C NMR (CD_3OD) *δ*: 21.28 (α-CH_3), 21.47 (C5′), 30.10 (C4′), 36.08 (CH_2), 39.10 (C3′), 45.71 (CH), 52.13 (C1′), 127.72 (Ar-C1), 128.67 (Ar-C4′), 128.99 (Ar-C2′), 129.04 (Ar-C3′), 130.67 (Ar-C6), 131.29 (Ar-C3), 138.38 (Ar-C2), 141.56 (Ar-C4), 143.12 (Ar-C4), 143.49 (Ar-C1′), 183.50 (CO_2Na), 223.14 (C=O). HR-FAB-MS (*m/z*): 367.1291 (M^++Na, calcd for

$C_{21}H_{21}Na_2O_3$: 367.1286). Anal. Calcd for $C_{21}H_{21}NaO_3 \cdot 0.5H_2O$: C, 71.22; H, 6.36. Found: C, 71.37, H, 6.27.

5.2.3.4. Sodium 2-{4′-methyl-5-[(2-oxocyclopentyl)methyl]]biphenyl-2-yl}propanoate (25). Yield: 77%, three steps. IR (KBr) *v*: 1420, 1712 (CO_2^-), 1733 (C=O), cm $^{-1}$. ^{1}H NMR (CD_3OD) *δ*: 1.21 (3H, dd, *J* = 7.3, 1.5 Hz, α-CH_3), 1.54–2.44 (7H, m, H1′, H3′, H4′, H5′), 2.36 (3H, s, Ar-CH_3), 2.51 (1H, dd, *J* = 13.4, 9.3 Hz, CH_2), 3.04 (1H, dd, *J* = 13.7, 9.3 Hz, CH_2), 3.72 (1H, q, *J* = 7.1 Hz, CH), 6.92 (1H, t, *J* = 1.8 Hz, Ar-H3), 7.08 (1H, dt, *J* = 8.1, 1.8 Hz, Ar-H5), 7.18 (2H, d, *J* = 7.7 Hz, Ar-H3′), 7.26 (2H, d, *J* = 7.7 Hz, Ar-H2′), 7.44 (1H, d, *J* = 8.1 Hz, Ar-H6). ^{13}C NMR (CD_3OD) *δ*: 21.19 (α-CH_3), 21.47 (C5′), 21.44 (C4′), 30.08 (Ar-CH_3), 36.07 (CH_2), 39.08 (C3′), 45.70 (CH), 52.12 (C1′), 128.61 (Ar-C1), 128.80 (Ar-C5), 129.58 (Ar-C2′), 130.53 (Ar-C3′), 131.31 (Ar-C6), 137.33 (Ar-C3), 138.29 (Ar-C4′), 140.52 (Ar-C2), 141.64 (Ar-C1′), 143.09 (Ar-C4), 183.58 (CO_2Na), 223.09 (C=O). HR-FAB-MS (*m/z*): 381.1439 (M^++Na, calcd for $C_{22}H_{23}Na_2O_3$: 381.1443). Anal. Calcd for $C_{22}H_{23}NaO_3 \cdot 0.5H_2O$: C, 72.03; H, 6.66. Found: C, 71.92, H, 6.58.

5.2.3.5. Sodium 2-{4′-methoxy-5-[(2-oxocyclopentyl)methyl]biphenyl-2-yl}propanoate (26). Yield: 70%, three steps. IR (KBr) *v*: 1416, 1711 (CO_2^-), 1732 (C=O), cm^{-1}. ^{1}H NMR (CD_3OD) *δ*: 1.22 (3H, dd, *J* = 7.0, 1.5 Hz, α-CH_3), 1.53–2.40 (7H, m, H1′, H3′, H4′, H5′), 2.51 (1H, dd, *J* = 13.6, 9.5 Hz, CH_2), 3.04 (1H, dd, *J* = 13.4, 3.8 Hz, CH_2), 3.73 (1H, q, *J* = 7.0 Hz, CH), 3.81 (3H, s, Ar-OCH_3), 6.92–6.95 (3H, m, Ar-H3, Ar-H3′), 7.07 (1H, d, *J* = 8.1 Hz, Ar-H5), 7.31 (2H, d, *J* = 8.4 Hz, Ar-H2′), 7.43 (1H, d, *J* = 8.1 Hz, Ar-H6). ^{13}C NMR (CD_3OD) *δ*: 21.23 (α-CH_3), 21.45 (C5′), 30.08 (C4′), 36.08 (CH_2), 39.09 (C3′), 45.70 (CH), 52.03 (C1′), 55.72 (Ar-OCH_3), 114.43 (Ar-C2′), 128.60 (Ar-C1), 128.72 (Ar-C5), 131.44 (Ar-C6), 131.70 (Ar-C3′), 135.81 (Ar-C3), 138.29 (Ar-C4′), 141.73 (Ar-C2), 142.78 (Ar-C1′), 160.07 (Ar-C4), 183.60 (CO_2Na), 223.10 (C=O). HR-FAB-MS (*m/z*): 397.1399 (M^++Na, calcd for $C_{22}H_{23}Na_2O_4$: 397.1392). Anal. Calcd for $C_{22}H_{23}NaO_4 \cdot H_2O$: C, 67.22; H, 6.38. Found: C, 67.33, H, 6.42.

5.2.3.6. Sodium 2-(4′-(methylthio)-5-((2-oxocyclopentyl)methyl)biphenyl-2-yl)propanoate (27). Yield: 60%, three steps. IR (KBr) *v*: 1417, 1712 (CO_2^-), 1730 (C=O), cm $^{-1}$. ^{1}H NMR (CD_3OD) *δ*: 1.23 (3H, dd, *J* = 7.1, 1.3 Hz, α-CH_3), 1.55–2.45 (7H, m, H1′, H3′, H4′, H5′), 2.49 (3H, s, Ar-SCH_3), 2.52 (1H, dd, *J* = 13.9, 9.2 Hz, CH_2), 3.05 (1H, dd, *J* = 13.6, 4.0 Hz, CH_2), 3.70 (1H, q, *J* = 7.2 Hz, CH), 6.94 (1H, t, *J* = 1.8 Hz, Ar-H3), 7.10 (1H, dt, *J* = 8.1, 2.2 Hz, Ar-H5), 7.31 (4H, dd, *J* = 14.5, 8.6 Hz, Ar-H2′, Ar-H3′), 7.45 (1H, d, *J* = 8.1 Hz, Ar-H6). ^{13}C NMR (CD_3OD) *δ*: 15.91 (Ar-SCH_3), 21.21 (α-CH_3), 21.45 (C5′), 30.09 (C4′), 36.06 (CH_2), 39.06 (C3′), 45.73 (CH), 52.12 (C1′), 127.36 (Ar-C3′), 128.70 (Ar-C1), 128.98 (Ar-C5), 129.05 (Ar-C6), 131.17 (Ar-C2′), 138.33 (Ar-C3), 138.44 (Ar-C2), 140.32 (Ar-C1′), 141.61 (Ar-C4), 142.49 (Ar-C4′), 183.42 (CO_2Na), 223.01 (C=O). HR-FAB-MS (*m/z*): 413.1165 (M^++Na, calcd for $C_{22}H_{23}Na_2SO_3$: 413.1163). Anal. Calcd for $C_{22}H_{23}NaSO_3 \cdot H_2O$: C, 64.54; H, 6.10. Found: C, 64.69, H, 6.17.

5.2.3.7. Sodium 2-{4′-fluoro-5-[(2-oxocyclopentyl)methyl]biphenyl-2-yl}propanoate (28). Yield: 64%, three steps. IR (KBr) *v*: 1204 (Ar-F), 1414, 1710 (CO_2^-), 1730 (C=O), cm^{-1}. ^{1}H NMR (CD_3OD) *δ*: 1.22 (3H, dd, *J* = 7.3, 1.1 Hz, α-CH_3), 1.55–2.41 (7H, m, H1′, H3′, H4′, H5′), 2.52 (1H, dd, *J* = 13.6, 9.2 Hz, CH_2), 3.05 (1H, dd, *J* = 13.6, 4.0 Hz, CH_2), 3.64 (1H, q, *J* = 7.2 Hz, CH), 6.93 (1H, t, *J* = 1.8 Hz, Ar-H3), 7.13–7.07 (3H, m, Ar-H5, Ar-H3′), 7.38–7.46 (3H, m, Ar-H6, Ar-H2′). ^{13}C NMR (CD_3OD) *δ*: 21.08 (α-CH_3), 21.45 (C5′), 30.09 (C4′), 36.04 (CH_2), 39.06 (C3′), 45.73 (CH), 52.09 (C1′), 115.60 (d, J_{C-F} = 21.1 Hz, Ar-C3′), 128.68 (Ar-C1), 129.19 (Ar-C5), 131.32 (Ar-C6), 132.46 (d, J_{C-F} = 8.1 Hz, Ar-C2′), 138.50 (Ar-C3), 139.57 (d, J_{C-F} = 3.7 Hz, Ar-C1′), 141.64 (Ar-C2), 142.02 (Ar-C4), 142.49 (d, J_{C-F} = 1.9 Hz, Ar-C4′), 183.28 (CO_2Na), 222.98 (C=O). HR-FAB-MS (*m/z*): 385.1188 (M^++Na, calcd for $C_{21}H_{20}FNa_2O_3$: 385.1192). Anal. Calcd for $C_{21}H_{20}FNaO_3 \cdot H_2O$: C, 66.31; H, 5.83. Found: C, 66.44, H, 5.76.

5.2.3.8. Sodium 2-{5-[(2-oxocyclopentyl)methyl]-4′-(trifluoromethoxy)biphenyl-2-yl}propanoate (29). Yield: 56%, three steps. IR (KBr) *v*: 1421, 1709 (CO_2^-), 1731 (C=O), cm $^{-1}$. ^{1}H NMR (CD_3OD) *δ*: 1.25 (3H, dd, *J* = 7.0, 1.1 Hz, α-CH_3), 1.51–2.45 (7H, m, H1′, H3′, H4′, H5′), 2.53 (1H, dd, *J* = 13.6, 9.5 Hz, CH_2), 3.05 (1H, dd, *J* = 13.6, 4.0 Hz, CH_2), 3.62 (1H, q, *J* = 7.2 Hz, CH), 6.95 (1H, t, *J* = 2.2 Hz, Ar-H3), 7.13 (1H, dt, *J* = 8.1, 2.2 Hz, Ar-H3′), 7.28 (2H, dd, *J* = 8.8, 0.7 Hz, Ar-H5,), 7.46–7.51 (3H, m, Ar-H6, Ar-H2′). ^{13}C NMR (CD_3OD) *δ*: 21.12 (α-CH_3), 21.44 (C5′), 30.08 (C4′), 35.99 (CH_2), 39.04 (C3′), 47.75 (CH), 52.04 (C1′), 121.51 (Ar-C3′), 128.77 (Ar-C1), 129.46 (Ar-C5), 131.17 (Ar-OCF_3), 131.23 (Ar-C6), 132.37 (Ar-C2′), 138.62 (Ar-C1′), 141.52 (Ar-C3), 141.57 (Ar-C2), 142.58 (Ar-C4),, 149.45 (Ar-C4′), 183.28 (CO_2Na), 222.98 (C=O). HR-FAB-MS (*m/z*): 451.1107 (M^++Na, calcd for $C_{22}H_{20}F_3Na_2O_4$: 451.1109). Anal. Calcd for $C_{22}H_{20}F_3NaO_4 \cdot 0.5H_2O$: C, 60.41; H, 4.84. Found: C, 60.34, H, 4.98.

5.2.3.9. Sodium 2′-(1-carboxylatoethyl)-5′-[(2-oxocyclopentyl)-methyl]biphenyl-4-carboxylate (30). Yield: 74%, three steps. IR (KBr) *v*: 1420, 1689, 1712 (CO_2^-), 1727 (C=O), cm $^{-1}$. ^{1}H NMR (CD_3OD) *δ*: 1.22 (3H, dd, *J* = 7.1, 1.6 Hz, α-CH_3), 1.33–2.42 (7H, m, H1′, H3′, H4′, H5′), 2.53 (1H, dd, *J* = 13.6, 9.2 Hz, CH_2), 3.06 (1H, dd, *J* = 13.6, 4.0 Hz, CH_2), 3.73 (1H, q, *J* = 7.1 Hz, CH), 6.96 (1H, st, *J* = 1.6 Hz, Ar-H3), 7.11 (1H, dt, *J* = 8.1, 1.8 Hz, Ar-H5), 7.40 (2H, d, *J* = 8.4 Hz, Ar-H2′), 7.44 (1H, d, *J* = 8.1 Hz, Ar-H6), 7.99 (2H, d, *J* = 8.4 Hz, Ar-H3′). ^{13}C NMR (CD_3OD) *δ*: 20.00 (α-CH_3), 21.45 (C5′), 30.11 (C4′), 36.06 (CH_2), 39.05 (C3′), 45.55 (CH), 52.11 (C1′), 128.64 (Ar-C1), 129.18 (Ar-C5′), 130.01 (Ar-C2′), 130.10 (Ar-C3′), 131.23 (Ar-C6), 137.37 (Ar-C3), 138.52 (Ar-C2), 141.47 (Ar-C4′), 142.81 (Ar-C4), 145.50 (Ar-C1′), 175.36 (Ar-CO_2Na), 183.17 (CO_2Na), 223.02 (C=O). HR-FAB-MS (*m/z*): 433.1001 (M^++Na, calcd for $C_{22}H_{20}Na_3O_5$: 433.1004). Anal. Calcd for $C_{22}H_{20}Na_2O_5 \cdot H_2O$: C, 61.68; H, 5.18. Found: C, 61.54, H, 5.06.

5.2.3.10. Sodium 2-{4′-hydroxy-5-[(2-oxocyclopentyl)methyl]-biphenyl-2-yl}propanoate (31). Yield: 50%, three steps. IR (KBr) *v*: 1318 (Ar-OH), 1421, 1710 (CO_2^-), 1731 (C=O), cm^{-1}. ^{1}H NMR (CD_3OD) *δ*: 1.22 (3H, dd, *J* = 7.3, 1.5 Hz, α-CH_3), 1.52–2.42 (7H, m, H1′, H3′, H4′, H5′), 2.50 (1H, d, *J* = 13.9 Hz, CH_2), 3.02 (1H, d, *J* = 13.6 Hz, CH_2), 3.75 (1H, q, *J* = 7.2 Hz, CH), 6.80 (2H, d, *J* = 8.4 Hz, Ar-H3′), 6.92 (1H, s, Ar-H3), 7.05 (1H, d, *J* = 8.1 Hz, Ar-H5), 7.21 (2H, d, *J* = 8.4 Hz, Ar-H2′), 7.42 (1H, d, *J* = 8.1 Hz, Ar-H6). ^{13}C NMR (CD_3OD) *δ*: 21.32 (α-CH_3), 30.10 (C5′), 36.10 (C4′), 39.09 (CH_2), 45.72 (C3′), 52.20 (CH), 58.31 (C1′), 116.15 (Ar-C3′), 128.40 (Ar-C1), 128.54 (Ar-C5), 131.51 (Ar-C6), 131.66 (Ar-C2′), 134.03 (Ar-C1′), 138.19 (Ar-C3), 141.76 (Ar-C2), 143.24 (Ar-C4), 158.47 (Ar-C4′), 183.81 (CO_2Na), 219.16 (C=O). HR-FAB-MS (*m/z*): 361.1414 (M^++H, calcd for $C_{21}H_{22}NaO_4$: 361.1416). Anal. Calcd for $C_{21}H_{21}NaO_4 \cdot H_2O$: C, 68.28; H, 6.00. Found: C, 68.30, H, 6.09.

5.2.4. Synthesis of the alcohol derivative of 31 (32, 33)

A methyl ester intermediate derived from **31** was reduced by $NaBH_4$ (see below) and alkaline hydrolyzed.

5.2.4.1. Reduction of methyl ester intermediate derived from 31 with $NaBH_4$. To a stirred solution of methyl ester intermediate derived from **31** (1 equiv, ca. 1.8 mmol) in EtOH, $NaBH_4$ (1.3 equiv, ca. 2.4 mmol) was added, stirred for 1 h at room temperature, quenched by the addition of a few ice chips, and the resulting solution was extracted with CH_2Cl_2. The extracts were dried over anhydrous Na_2SO_4 and filtrated. The filtrate was evaporated to

dryness, and the mixture was separated into *cis*-alcohol and *trans*-alcohol as two kinds of colorless oil by silica gel chromatography (*n*-hexane/AcOEt, 7:2) (93–95%).

5.2.4.2. (±)-2-{4′-Hydroxy-5-[(trans-2-hydroxycyclopentyl)methyl]biphenyl-2-yl}propanoic acid (32). Yield: 82%, three steps. IR (KBr) *ν*: 1321 (Ar-OH), 1421, 1714 (CO_2^-), 1733 (C=O), 3466 (OH), cm^{-1}. ^1H NMR (CD_3OD) *δ*: 1.27 (3H, d, *J* = 7.1 Hz, α-CH_3), 1.20–1.94 (6H, m, H3′, H4′, H5′), 1.95–2.06 (1H, m, H1′), 2.38 (1H, dd, *J* = 13.6, 9.2 Hz, CH_2), 2.85 (1H, dd, *J* = 13.6, 5.7 Hz, CH_2), 3.78–3.88 (2H, m, CH, H2′), 6.83 (2H, d, *J* = 8.4 Hz, Ar-H3′), 7.00 (1H, s, Ar-H3), 7.11–7.16 (3H, m, Ar-H5, Ar-H2′), 7.27 (1H, d, *J* = 8.1 Hz, Ar-H6), 10.57 (1H, br s, CO_2H). ^{13}C NMR (CD_3OD) *δ*: 19.72 (α-CH_3), 22.37 (C4′), 30.30 (C5′), 34.64 (CH_2), 40.11 (C3′), 42.04 (CH), 50.67 (C1′), 78.83 (C2′), 115.94 (Ar-C3′), 127.66 (Ar-C1), 128.98 (Ar-C5), 131.55 (Ar-C6), 131.88 (Ar-C3), 133.97 (Ar-C1′), 137.99 (Ar-C2′), 140.95 (Ar-C2), 143.03 (Ar-C4), 157.73 (Ar-C4′), 178.94 (CO_2H). HR-FAB-MS (*m/z*): 340.1677 (M^+, calcd for $C_{21}H_{24}O_4$: 340.1675). Anal. Calcd for $C_{21}H_{24}O_4 \cdot 0.25H_2O$: C, 73.13; H, 7.16. Found: C, 72.91, H, 7.30.

5.2.4.3. (±)-2-{4′-Hydroxy-5-[(*cis*-2-hydroxycyclopentyl)methyl]-biphenyl-2-yl}propanoic acid (33). Yield: 80%, three steps. IR (KBr) *ν*: 1318 (Ar-OH), 1420, 1714 (CO_2^-), 1731 (C=O), 3466 (OH), cm^{-1}. ^1H NMR (CD_3OD) *δ*: 1.27 (3H, d, *J* = 7.0 Hz, α-CH_3), 1.44–1.87 (6H, m, H3′, H4′, H5′), 1.90–2.02 (1H, m, H1′), 2.56 (1H, dd, *J* = 13.4, 8.2 Hz, CH_2), 2.87 (1H, dd, *J* = 6.8, 3.4 Hz, CH_2), 3.85 (1H, q, *J* = 7.1 Hz, CH), 4.04 (1H, br s, H2′), 6.80 (2H, d, *J* = 8.4 Hz, Ar-H3′), 7.04 (1H, s, Ar-H3), 7.15 (3H, d, *J* = 8.4 Hz, Ar-H5, Ar-H2′), 7.26 (1H, d, *J* = 8.1 Hz, Ar-H6), 10.56 (1H, br s, CO_2H). ^{13}C NMR (CD_3OD) *δ*: 19.37 (α-CH_3), 22.56 (C4′), 29.62 (C5′), 35.41 (CH_2), 36.07 (C3′), 42.03 (CH), 50.67 (C1′), 75.18 (C2′), 115.92 (Ar-C3′), 127.60 (Ar-C1), 128.89 (Ar-C5), 131.56 (Ar-C6), 131.79 (Ar-C3), 134.07 (Ar-C1′), 137.77 (Ar-C2′), 141.84 (Ar-C2), 142.98 (Ar-C4), 157.69 (Ar-C4′), 178.99 (CO_2H). HR-FAB-MS (*m/z*): 340.1678 (M^+, calcd for $C_{21}H_{24}O_4$: 340.1675). Anal. Calcd for $C_{21}H_{24}O_4 \cdot 0.5H_2O$: C, 72.18; H, 7.21. Found: C, 72.35, H, 7.29.

5.3. Membrane permeability assay

Permeabilization of calcein-loaded liposomes was assayed as described previously,[14] with some modifications. Liposomes were prepared using the reversed-phase evaporation method. Egg phosphatidylcholine (PC) (10 μmol, 7.7 mg) was dissolved in chloroform/methanol (1:2, v/v), dried, dissolved in 1.5 mL of diethyl ether, and added to 1 mL of 100 mM calcein/NaOH (pH 7.4). The mixture was then sonicated to obtain a homogenous emulsion. The diethyl ether solvent was removed and the resulting suspension of liposomes was centrifuged and washed twice with fresh buffer A (10 mM phosphate buffer (Na_2HPO_4–NaH_2PO_4) (pH 6.8) containing 150 mM NaCl) to remove untrapped calcein. The final liposome precipitate was re-suspended in 5 mL buffer A. A 30 μL aliquot of this suspension was diluted with buffer A to 20 mL, and 12 or 400 μL of this diluted suspension was then incubated at 30 °C for 10 min in the presence of the compound under investigation. Control experiments were performed after addition of the same volume of water. The release of calcein from liposomes was determined by measuring the fluorescence intensity at 520 nm (excitation at 490 nm).

5.4. Human whole blood COX assay

This assay was performed as decribed[43] with some modifications. Fresh blood was collected in tubes (Protein Lobinding tube, Eppendorf Co., Ltd, Tokyo, Japan) by venipuncture from healthy volunteers who had no apparent inflammatory conditions and had not taken any NSAIDs for least 7 days prior to blood collection.

5.4.1. COX-1 assay

Aliquots of blood (500 μL) were incubated with 2 μL of test compound for 24 h at 37 °C, then centrifuged to obtain plasma. Aliquots (100 μL) of plasma were mixed with 400 μL methanol and centrifuged. The amount of TXB_2 in the supernatant was determined using an EIA kit (Cayman, Ann Arbor, MI) according to the manufacturer's protocol.

5.4.2. COX-2 assay

Blood samples (500 μL) were incubated with 100 μg/mL lipopolysaccharide (Sigma–Aldrich Japan Inc., Tokyo, Japan) for 24 h at 37 °C after addition of 2 μL of test compound, then centrifuged to obtain plasma. Aliquots (100 μL) of plasma were mixed with 400 μL methanol and centrifuged. The amount of PGE_2 in the supernatant was determined using an EIA kit (Cayman, Ann Arbor, MI) according to the manufacturer's protocol.

5.5. Gastric damage assay and determination of gastric level of PGE_2

Wistar rats (6 weeks old, 180–200 g, male) were obtained from Kyudo Co., Ltd (Kumamoto, Japan). The experiments and procedures described here were carried out in accordance with the Guide for the Care and Use of Laboratory Animals as adopted and promulgated by the National Institutes of Health (Bethesda, MD), and were approved by the Animal Care Committee of Kumamoto University.

The gastric ulcerogenic response was examined as described previously,[20] with some modifications. Rats fasted for 18 h were orally administered NSAIDs. Eight hours later, the animals were sacrificed, after which their stomachs were removed and the areas of gastric mucosal lesions were measured by an observer unaware of the treatment they had received. Calculation of the scores involved measuring the area of all the lesions in square millimeters and summing the values to give an overall gastric lesion index. The gastric PGE_2 level was determined by EIA according to the manufacturer's instructions.

5.6. Carrageenan-induced rat paw edema

This assay was carried out as described previously.[44] Rats were orally administered NSAIDs and 1 h later received a 100 μL intradermal injection of carrageenan (1%) into the left hindpaw. Paw volume was measured using a plethsysmometer, which measures water displacement when the paw is submerged in a water cell. The percentage difference in volume between both paws was shown as edema (%). The PGE_2 level in the paw was determined by EIA according to the manufacturer's instructions.

5.7. Statistical analysis

All values are expressed as the mean ± SEM. The Tukey test or the Student's *t*-test for unpaired results was used to evaluate differences between more than three groups or between two groups, respectively. Differences were considered to be significant for values of $P < 0.05$.

Acknowledgments

This work was supported by Grants-in-Aid of Scientific Research from the Ministry of Health, Labour, and Welfare of Japan, Grants-in-Aid for Scientific Research from the Ministry of

Education, Culture, Sports, Science and Technology of Japan, and Grants-in-Aid of the Japan Science and Technology Agency.

Supplementary data

Supplementary data (NMR spectra of final compounds) associated with this article can be found, in the online version, at doi:10.1016/j.bmc.2011.04.050.

References and notes

1. Smalley, W. E.; Ray, W. A.; Daugherty, J. R.; Griffin, M. R. *Am. J. Epidemiol.* **1995**, *141*, 539.
2. Singh, G. *Am. J. Med.* **1998**, *105*, 31S.
3. Kujubu, D. A.; Fletcher, B. S.; Varnum, B. C.; Lim, R. W.; Herschman, H. R. *J. Biol. Chem.* **1991**, *266*, 12866.
4. Xie, W. L.; Chipman, J. G.; Robertson, D. L.; Erikson, R. L.; Simmons, D. L. *Proc. Natl. Acad. Sci. U.S.A.* **1991**, *88*, 2692.
5. Silverstein, F. E.; Faich, G.; Goldstein, J. L.; Simon, L. S.; Pincus, T.; Whelton, A.; Makuch, R.; Eisen, G.; Agrawal, N. M.; Stenson, W. F.; Burr, A. M.; Zhao, W. W.; Kent, J. D.; Lefkowith, J. B.; Verburg, K. M.; Geis, G. S. *JAMA* **2000**, *284*, 1247.
6. Bombardier, C.; Laine, L.; Reicin, A.; Shapiro, D.; Burgos, V. R.; Davis, B.; Day, R.; Ferraz, M. B.; Hawkey, C. J.; Hochberg, M. C.; Kvien, T. K.; Schnitzer, T. J. N. *Engl. J. Med.* **2000**, *343*, 1520.
7. FitzGerald, G. A.; Patrono, C. N. *Engl. J. Med.* **2001**, *345*, 433.
8. Mukherjee, D.; Nissen, S. E.; Topol, E. J. *JAMA* **2001**, *286*, 954.
9. Mukherjee, D. *Biochem. Pharmacol.* **2002**, *63*, 817.
10. Juni, P.; Nartey, L.; Reichenbach, S.; Sterchi, R.; Dieppe, P. A.; Egger, M. *Lancet* **2004**, *364*, 2021.
11. Lichtenberger, L. M. *Biochem. Pharmacol.* **2001**, *61*, 631.
12. Tanaka, K.; Tomisato, W.; Hoshino, T.; Ishihara, T.; Namba, T.; Aburaya, M.; Katsu, T.; Suzuki, K.; Tsutsumi, S.; Mizushima, T. *J. Biol. Chem.* **2005**, *280*, 31059.
13. Tsutsumi, S.; Gotoh, T.; Tomisato, W.; Mima, S.; Hoshino, T.; Hwang, H. J.; Takenaka, H.; Tsuchiya, T.; Mori, M.; Mizushima, T. *Cell Death Differ.* **2004**, *11*, 1009.
14. Tomisato, W.; Tanaka, K.; Katsu, T.; Kakuta, H.; Sasaki, K.; Tsutsumi, S.; Hoshino, T.; Aburaya, M.; Li, D.; Tsuchiya, T.; Suzuki, K.; Yokomizo, K.; Mizushima, T. *Biochem. Biophys. Res. Commun.* **2004**, *323*, 1032.
15. Tomisato, W.; Tsutsumi, S.; Rokutan, K.; Tsuchiya, T.; Mizushima, T. *Am J. Physiol. Gastrointest. Liver Physiol.* **2001**, *281*, G1092.
16. Aburaya, M.; Tanaka, K.; Hoshino, T.; Tsutsumi, S.; Suzuki, K.; Makise, M.; Akagi, R.; Mizushima, T. *J. Biol. Chem.* **2006**, *281*, 33422.
17. Tsutsumi, S.; Namba, T.; Tanaka, K. I.; Arai, Y.; Ishihara, T.; Aburaya, M.; Mima, S.; Hoshino, T.; Mizushima, T. *Oncogene* **2006**, *25*, 1018.
18. Namba, T.; Hoshino, T.; Tanaka, K.; Tsutsumi, S.; Ishihara, T.; Mima, S.; Suzuki, K.; Ogawa, S.; Mizushima, T. *Mol. Pharmacol.* **2007**, *71*, 860.
19. Ishihara, T.; Hoshino, T.; Namba, T.; Tanaka, K.; Mizushima, T. *Biochem. Biophys. Res. Commun.* **2007**, *356*, 711.
20. Tomisato, W.; Tsutsumi, S.; Hoshino, T.; Hwang, H. J.; Mio, M.; Tsuchiya, T.; Mizushima, T. *Biochem. Pharmacol.* **2004**, *67*, 575.
21. Misaka, E.; Yamaguchi, T.; Iizuka, Y.; Kamoshida, K.; Kojima, T.; Kobayashi, K.; Endo, Y.; Misawa, Y.; Lobayashi, S.; Tanaka, K. *Pharmacometrics* **1981**, *21*, 753.
22. Kawano, S.; Tsuji, S.; Hayashi, N.; Takei, Y.; Nagano, K.; Fusamoto, H.; Kamada, T. *J. Gastroenterol. Hepatol.* **1995**, *10*, 81.
23. Sugimoto, M.; Kojima, T.; Asami, M.; Iizuka, Y.; Matsuda, K. *Biochem. Pharmacol.* **1991**, *42*, 2363.
24. Yamakawa, N.; Suemasu, S.; Kimoto, A.; Arai, Y.; Ishihara, T.; Yokomizo, K.; Okamoto, Y.; Otsuka, M.; Tanaka, K.; Mizushima, T. *Biol. Pharm. Bull.* **2010**, *33*, 398.
25. Yamakawa, N.; Suemasu, S.; Matoyama, M.; Kimoto, A.; Takeda, M.; Tanaka, K.; Ishihara, T.; Katsu, T.; Okamoto, Y.; Otsuka, M.; Mizushima, T. *J. Med. Chem.* **2010**, *53*, 7879.
26. Miyaura, N.; Suzuki, A. *Chem. Rev.* **1995**, *95*, 2457.
27. Stanforth, S. P. *Tetrahedron* **1998**, *54*, 263.
28. Kurumbail, R. G.; Stevens, A. M.; Gierse, J. K.; McDonald, J. J.; Stegeman, R. A.; Pak, J. Y.; Gildehaus, D.; Miyashiro, J. M.; Penning, T. D.; Seibert, K.; Isakson, P. C.; Stallings, W. C. *Nature* **1996**, *384*, 644.
29. Loll, P. J.; Picot, D.; Ekabo, O.; Garavito, R. M. *Biochemistry* **1996**, *35*, 7330.
30. Loll, P. J.; Picot, D.; Garavito, R. M. *Nat. Struct. Biol.* **1995**, *2*, 637.
31. Luong, C.; Miller, A.; Barnett, J.; Chow, J.; Ramesha, C.; Browner, M. F. *Nat. Struct. Biol.* **1996**, *3*, 927.
32. Mengle-Gaw, L. J.; Schwartz, B. D. *Mediators. Inflamm.* **2002**, *11*, 275.
33. Sekiguchi, M.; Shirasaka, M.; Konno, S.; Kikuchi, S. B. M. C. *Musculoskelet Disord.* **2008**, *9*, 15.
34. Anana, R.; Rao, P. N.; Chen, Q. H.; Knaus, E. E. *Bioorg. Med. Chem.* **2006**, *14*, 5259.
35. Zarghi, A.; Zebardast, T.; Hakimion, F.; Shirazi, F. H.; Rao, P. N.; Knaus, E. E. *Bioorg. Med. Chem.* **2006**, *14*, 7044.
36. Goto, J.; Kataoka, R.; Muta, H.; Hirayama, N. *J. Chem. Inf. Model.* **2008**, *48*, 583.
37. McAdam, B. F.; Catella, L. F.; Mardini, I. A.; Kapoor, S.; Lawson, J. A.; FitzGerald, G. A. *Proc. Natl. Acad. Sci. U.S.A.* **1999**, *96*, 272.
38. Catella, L. F.; McAdam, B.; Morrison, B. W.; Kapoor, S.; Kujubu, D.; Antes, L.; Lasseter, K. C.; Quan, H.; Gertz, B. J.; FitzGerald, G. A. *J. Pharmacol. Exp. Ther.* **1999**, *289*, 735.
39. Belton, O.; Byrne, D.; Kearney, D.; Leahy, A.; Fitzgerald, D. J. *Circulation* **2000**, *102*, 840.
40. Kvern, B. *Can. Fam. Physician* **2002**, *48*, 1449.
41. Esser, R.; Berry, C.; Du, Z.; Dawson, J.; Fox, A.; Fujimoto, R. A.; Haston, W.; Kimble, E. F.; Koehler, J.; Peppard, J.; Quadros, E.; Quintavalla, J.; Toscano, K.; Urban, L.; van Duzer, J.; Zhang, X.; Zhou, S.; Marshall, P. J. *Br. J. Pharmacol.* **2005**, *144*, 538.
42. Ushiyama, S.; Yamada, T.; Murakami, Y.; Kumakura, S.; Inoue, S.; Suzuki, K.; Nakao, A.; Kawara, A.; Kimura, T. *Eur. J. Pharmacol.* **2008**, *578*, 76.
43. Brideau, C.; Kargman, S.; Liu, S.; Dallob, A. L.; Ehrich, E. W.; Rodger, I. W.; Chan, C. C. *Inflamm. Res.* **1996**, *45*, 68.
44. Biddlestone, L.; Corbett, A. D.; Dolan, S. *Br. J. Pharmacol.* **2007**, *151*, 285.

British Journal of Nutrition (2011), **106**, 475–485
doi:10.1017/S0007114511000365

Protective effect of β-(1,3 → 1,6)-D-glucan against irritant-induced gastric lesions

Ken-ichiro Tanaka[1], Yuta Tanaka[1], Toshio Suzuki[2] and Tohru Mizushima[1]*

[1]*Graduate School of Medical and Pharmaceutical Sciences, Kumamoto University, 5-1 Oe-honmachi, Kumamoto 862-0973, Japan*

[2]*Research and Development, Daiso Company Limited, Amagasaki 660-0842, Japan*

(Received 17 August 2010 – Revised 18 November 2010 – Accepted 20 December 2010 – First published online 29 March 2011)

Abstract

β-(1,3)-D-Glucan with β-(1,6) branches has been reported to have various pharmacological activities, such as anti-tumour and anti-infection activities, which result from its immunomodulating effects. Gastric lesions result from an imbalance between aggressive and defensive factors. In the present study, we examined the effect of β-(1,3)-D-glucan with β-(1,6) branches isolated from *Aureobasidium pullulans* on the gastric ulcerogenic response in mice. Oral administration of β-glucan ameliorated gastric lesions induced by ethanol (EtOH) or HCl. This administration of β-glucan also suppressed EtOH-induced inflammatory responses, such as infiltration of neutrophils and expression of pro-inflammatory cytokines, chemokines and cell adhesion molecules (CAM) at the gastric mucosa. Of the various defensive factors, the levels of heat shock protein (HSP) 70 and mucin but not PGE_2 were increased by the administration of β-glucan. β-Glucan-dependent induction of the expression of HSP70 and mucin proteins and suppression of the expression of pro-inflammatory cytokines, chemokines and CAM were also observed in cultured cells *in vitro*. The results of the present study suggest that β-glucan protects the gastric mucosa from the formation of irritant-induced lesions by increasing the levels of defensive factors, such as HSP70 and mucin.

Key words: β-(1,3 → 1,6)-D-Glucan: Gastric lesions: Heat shock protein 70: Mucin: Ethanol

The balance between aggressive and defensive factors determines whether gastric lesions develop, with either a relative increase in aggressive factors or a relative decrease in defensive factors resulting in lesions. The gastric mucosa is challenged by a variety of both endogenous and exogenous irritants (aggressive factors), including ethanol (EtOH), gastric acid, pepsin, reactive oxygen species and non-steroidal anti-inflammatory drugs[1]. In order to protect the gastric mucosa against these aggressive factors, a complex defence system, which includes the production of surface mucus (gastric mucin) and bicarbonate and the regulation of gastric mucosal blood flow, has evolved. PG, in particular PGE_2, enhance these protective mechanisms, and are therefore thought to be a major gastric mucosal defensive factor[2].

Recently, heat shock proteins (HSP) have also attracted considerable attention as another important defensive factor. When cells are exposed to stressors, HSP are induced in a manner that is dependent on the transcription factor heat shock factor 1 (HSF1), and this cellular up-regulation, in particular the up-regulation of HSP70, provides resistance to such stressors[3–6]. We have recently reported that HSF1-null mice or transgenic mice expressing HSP70 show sensitive or resistant phenotypes, respectively, to irritant-induced gastric lesions[7,8], suggesting that HSP, especially HSP70, play an important role in the protection of the gastric mucosa against irritant-induced gastric lesions.

Chemicals that decrease the level of aggressive factors or increase the level of defensive factors are beneficial for protecting the gastric mucosa against the formation of irritant-induced lesions. Acid-control drugs, such as histamine-2 receptor antagonists and proton pump inhibitors, and anti-*Helicobacter pylori* drugs belong to the former group, while drugs that induce the production of gastric mucins, PG and HSP belong to the latter. These chemicals (anti-ulcer drugs) decrease the incidence of surgery for the treatment of gastric ulcers, resulting in a good quality of life for patients with this disease. However, in order to decrease healthcare costs and to prevent the development of gastric ulcers, it is important to find health foods and supplements (complementary and alternative medicines) that can reduce the level of aggressive factors or increase the level of defensive factors.

Abbreviations: CAM, cell adhesion molecule; EtOH, ethanol; HSF1, heat shock factor 1; HSP, heat shock protein; LMW β-glucan, low-molecular-weight β-(1,3 → 1,6)-D-glucan; MPO, myeloperoxidase.

***Corresponding author:** Dr T. Mizushima, email mizu@gpo.kumamoto-u.ac.jp

British Journal of Nutrition

β-Glucans are naturally occurring polysaccharides found in the cell walls of yeast, fungi, cereal plants and certain bacteria[9,10]. As suggested by the fact that various foods contain β-glucans, they are known to have little toxic and adverse effects[9]. β-Glucans from fungi occur as β-(1,3)-linked glucose polymers with β-(1,6) side chains of varying length and distribution[9–11]. Such β-glucans from mushrooms have been used as anti-tumour drugs in Japan[10]. They are thought to achieve anti-tumour effects through their immunoactivating activities, such as stimulating the release of cytokines, NO and arachidonic acid metabolites[10–14]. In addition, β-(1,3)-D-glucans with β-(1,6) branches have been reported to have various other beneficial effects, such as enhancing defence against bacterial, viral, fungal and parasitic challenge, increasing haematopoiesis and radioprotection, stimulating the wound-healing response, and decreasing the levels of serum lipids[9,10,15,16]. Interestingly, it has recently been reported that β-glucans suppress inflammatory responses in some animal models by decreasing the levels of pro-inflammatory cytokines, chemokines and cell adhesion molecules (CAM)[17–22]. This suggests that β-glucan is an interesting immunomodulator, causing opposing effects on immune systems. Since the cytoprotective effects of β-glucans and suppression by β-glucans of anti-tumour drug-induced damage in the small intestine have been reported[17,23,24], it is possible that β-glucans protect against the formation of irritant-induced gastric lesions. However, no studies have examined this possibility to date.

We have used β-(1,3)-D-glucan with β-(1,6) branches isolated from *Aureobasidium pullulans*[14,25]. In general, β-(1,3)-D-glucans with β-(1,6) branches have a high molecular weight (over 2000 kDa), high viscosity and low water solubility. In addition, such β-glucans easily form gels containing high-order structures of single or triplet spirals. Therefore, its purification is extremely difficult and, in previous studies, crude β-glucan fractions rather than purified ones have been used in experiments[9]. We succeeded in the purification and industrial-scale production of low-molecular-weight β-(1,3 → 1,6)-D-glucan (LMW β-glucan) from the *A. pullulans* GM-NH-1A1 strain (black yeast, a mutant strain K-1)[14]. The characteristic features of this β-glucan are its LMW (about 100 kDa), low viscosity, high water solubility and high level of β-(1-6) branching (50–80 %)[14,25]. We have previously reported that LMW β-glucan has various clinically beneficial effects, such as suppression of the allergic response by increasing the levels of IL-12 and interferon-γ; suppression of restraint stress-induced immunosuppression (such as suppression of natural killer cell activity and IL-12 and IL-6 production); anti-tumour and anti-metastatic actions mediated via stimulation of the immune system in the small intestine; and protective effects against anti-tumour drug-induced damage in the small intestine[14,23,25,26]. In the present study, we found that LMW β-glucan protects the gastric mucosa of mice against the formation of irritant-induced lesions. We also suggest that LMW β-glucan achieves this gastroprotective effect by increasing the levels of defensive factors, such as HSP70 and gastric mucin.

Materials and methods

Chemicals and animals

LMW β-glucan was prepared from the conditioned culture medium of *A. pullulans* GM-NH-1A1, as described previously[14,25]. Analysis of ^{1}H and ^{13}C NMR spectra and gel-filtration chromatography revealed that LMW β-glucan has approximately 70 % β-(1-6) branches and an average molecular weight of 100 kDa, as described previously[14,25]. Lipopolysaccharide, U0126 (an inhibitor of extracellular signal-regulated kinase), paraformaldehyde, peroxidase standard, fetal bovine serum, *o*-dianisidine and hexadecyl trimethyl ammonium bromide were obtained from Sigma (St Louis, MO, USA). α-(1,4 → 1,6)-D-Glucan (pullulan, molecular weight 50 000–100 000) was obtained from WAKO Pure Chemicals (Tokyo, Japan). Terminal deoxynucleotidyl transferase was obtained from Toyobo (Osaka, Japan). SB203580 (an inhibitor of p38 mitogen-activated protein kinase (p38)), SP600125 (an inhibitor of c-jun NH_2-terminal kinase) and the ELISA kit for detection of PGE_2 were from Cayman Chemicals (Ann Arbor, MI, USA). Biotin 14-ATP and Alexa Fluor 488 conjugated with streptavidin were purchased from Invitrogen (Carlsbad, CA, USA). Mounting medium for immunohistochemical analysis (VECTASHIELD) was from Vector Laboratories (Burlingame, CA, USA). The RNeasy kit was obtained from Qiagen (Valencia, CA, USA), the PrimeScript® 1st strand cDNA Synthesis Kit was from TAKARA Bio (Ohtsu, Japan) and the iQ SYBR Green Supermix was from Bio-Rad (Hercules, CA, USA). Mayer's haematoxylin, 1 % eosin alcohol solution, cold Schiff's reagent, sulphate solution, 1 % periodic acid solution and mounting medium for histological examination (malinol) were from MUTO Pure Chemicals (Tokyo, Japan). The compound 4,6-diamino-2-phenylindole was from Dojindo (Kumamoto, Japan). Antibodies against HSP70 (for immunohistochemical analysis) and dectin-1 were from R&D Systems (Minneapolis, MN, USA). An antibody against HSP70 (for immunoblotting analysis) was from Stressgen (Ann Arbor, MI, USA), while one against HSF1 was kindly provided by Dr Akira Nakai (Yamaguchi University, Yoshida, Japan).

Wild-type ICR mice (6–8 weeks old, male) were used. The experiments and procedures described here were carried out in accordance with the Guide for the Care and Use of Laboratory Animals as adopted and promulgated by the National Institute of Health, and were approved by the Animal Care Committee of Kumamoto University (Kumamoto, Japan).

Gastric damage assay

Gastric ulcerogenic response was examined as described previously[7]. Mice, which had been fasted for 18 h, were orally administered either EtOH or HCl (5 ml/kg). After 4 h, the animals were killed with an overdose of diethyl ether, after which their stomachs were removed and scored for haemorrhagic damage by an observer unaware of the treatment they had received. Calculation of the scores involved measuring the area of all lesions in millimetres squared and summing the values to give an overall gastric lesion index. Gastric mucosal PGE_2 levels were determined by ELISA, as described previously[27].

Histopathological and immunohistochemical analyses and terminal deoxynucleotidyl transferase dUTP nick-end labelling assay

Gastric tissue samples were fixed in 4% buffered paraformaldehyde, and then embedded in paraffin before being cut into 4 μm-thick sections.

For histopathological examination, sections were stained first with Mayer's haematoxylin and then with 1% eosin alcohol solution (haematoxylin and eosin staining). Samples were mounted with malinol and inspected with the aid of an Olympus BX51 microscope (Tokyo, Japan).

For immunohistochemical analysis, sections were incubated with 0·3% H_2O_2 in methanol for the removal of endogenous peroxidase. Sections were blocked with 2·5% goat serum for 10 min, incubated for 12 h with an antibody against HSP70 (1:40 dilution) in the presence of 2·5% bovine serum albumin and then incubated for 2 h with a peroxidase-labelled polymer conjugated to goat anti-mouse Ig. Then, 3,3′-diaminobenzidine was applied to the sections, and the sections were finally incubated with Mayer's haematoxylin. Samples were mounted with malinol and inspected using a fluorescence microscope (Olympus BX51).

For the terminal deoxynucleotidyl transferase dUTP nick-end labelling assay, sections were incubated first with proteinase K (20 μg/ml) for 15 min at 37°C, then with TdTase and biotin 14-ATP for 1 h at 37°C and finally with Alexa Fluor 488 conjugated with streptavidin and 4,6-diamino-2-phenylindole for 2 h. Samples were mounted with VECTASHIELD and inspected with the aid of a fluorescence microscope (Olympus BX51).

Periodic acid Schiff staining

Gastric tissue samples were fixed in Carnoy's fluid (EtOH–acetic anhydride 3:1), and embedded in paraffin before being cut into 4 μm-thick sections. Sections were incubated with 1% periodic acid solution for 10 min, then with cold Schiff's reagent for 15 min and finally with sulphate solution for 2 min. Sections were incubated with Mayer's haematoxylin, mounted with malinol and inspected using a fluorescence microscope (Olympus BX51).

Real-time RT-PCR analysis

Real-time RT-PCR was performed as described previously[28], with some modifications. Total RNA was extracted using an RNeasy kit according to the manufacturer's protocol. Samples (2·5 μg RNA) were reverse-transcribed using the PrimeScript® 1st strand cDNA Synthesis Kit. Synthesised complementary DNA was used in real-time RT-PCR (Chromo 4 instrument; Bio-Rad) experiments using the iQ SYBR GREEN Supermix, and analysed with Opticon Monitor Software (Bio-Rad). Specificity was confirmed by electrophoretic analysis of the reaction products and by inclusion of template- or RT-free controls. To normalise the amount of total RNA present in each reaction, *gapdh* or *actin* complementary DNA was used as an internal standard.

Primers were designed using the Primer3 website. The primers used were as follows (name: forward primer, reverse primer). For humans, *muc-1*: 5′-acacaaacccagcagtggc-3′, 5′-actcagctcagcggcgac-3′; *muc-5ac*: 5′-cagccacgtccccttcaata-3′, 5′-accgcatttgggcatcc-3′; *actin*: 5′-ggacttcgagcaagagatgg-3′, 5′-agcactgtgttggcgtacag-3′. For mice, *tnf-α*: 5′-cgtcagccgatttgctatct-3′, 5′-cggactccgcaaagtctaag-3′; *il-1β*: 5′-gatcccaagcaatacccaaa-3′, 5′-ggggaactctgcagactcaa-3′; *il-6*: 5′-ctggagtcacagaaggagtgg-3′, 5′-ggtttgccgagtagatctcaa-3′; macrophage inflammatory protein (*mip*)-*2α*: 5′-accctgccaagggttgacttc-3′, 5′-ggcacatcaggtacgatccag-3′; monocyte chemoattractant protein (*mcp*)-*1*: 5′-ctcacctgctgctactcattc-3′, 5′-gcttgaggtggttgtggaaaa-3′; vascular cell adhesion molecule (*vcam*)-*1*: 5′-ctcctgcacttgtggaaatg-3′, 5′-tgtacgagccatccacagac-3′; intercellular adhesion molecule (*icam*)-*1*: 5′-tcgtgatggcagcctcttat-3′, 5′-gggcttgtcccttgagtttt-3′; *muc-1*: 5′-gccttcagtgccaagtcaat-3′, 5′-gaaggagaccccaacagaca-3′; *muc-5ac*: 5′-aaagacaccagtagtcactcagcaa-3′, 5′-ctgggaagtcagtgtcaaacca-3′; *gapdh*: 5′-aactttggcattgtggaagg-3′, 5′-acacattgggggtaggaaca-3′.

Myeloperoxidase activity

Myeloperoxidase (MPO) activity in the gastric tissues was measured as described previously[29,30]. Animals were placed under deep diethyl ether anaesthesia and killed. Stomachs were dissected, rinsed with cold saline and cut into small pieces. Samples were homogenised, freeze-thawed and centrifuged. The protein concentrations of the supernatants were determined using the Bradford method[31]. MPO activity was determined in 10 mM-phosphate buffer with 0·5 mM-*o*-dianidisine, 0·00 005% (w/v) H_2O_2 and 20 μg protein. MPO activity was obtained from the slope of the reaction curve, and its specific activity was expressed as the number of H_2O_2 molecules converted/min per mg protein.

Preparation of mouse peritoneal macrophages

Mouse peritoneal macrophages were prepared as described previously[32]. Mice were given 2 ml of 10% proteose peptone by intraperitoneal injection and peritoneal cells were harvested 3 d later. The cells were seeded in 60 mm culture dishes. After incubation for 4 h, non-adherent cells were removed and the adherent cells were cultured for use in the experiments. Virtually, all of the adherent cells were macrophages, as described previously[33].

Cell culture and immunoblotting analysis

Human gastric carcinoma cells were cultured in RPMI-1640 medium supplemented with 10% fetal bovine serum, penicillin (100 μg/ml) and streptomycin (100 μg/ml) in a humidified atmosphere of 95% air with 5% CO_2 at 37°C.

Whole-cell extracts were prepared as described previously[34]. The protein concentration of the samples was determined by the Bradford method[31]. Samples were applied to polyacrylamide SDS gels and subjected to electrophoresis, and the resultant proteins were immunoblotted with an antibody for HSP70 or actin.

Statistical analysis

All values are expressed as means with their standard errors. Two-way ANOVA followed by the Tukey test or Student's *t* test for unpaired results was used to evaluate differences between more than three groups or between two groups, respectively. Differences were considered to be significant for values of $P<0{\cdot}05$.

Results

Effect of low-molecular-weight β-(1,3 → 1,6)-D-glucan on gastric ulcerogenic and inflammatory responses

The effect of oral pre-administration of LMW β-glucan on the development of gastric lesions following oral administration of EtOH was examined in mice. We have previously reported

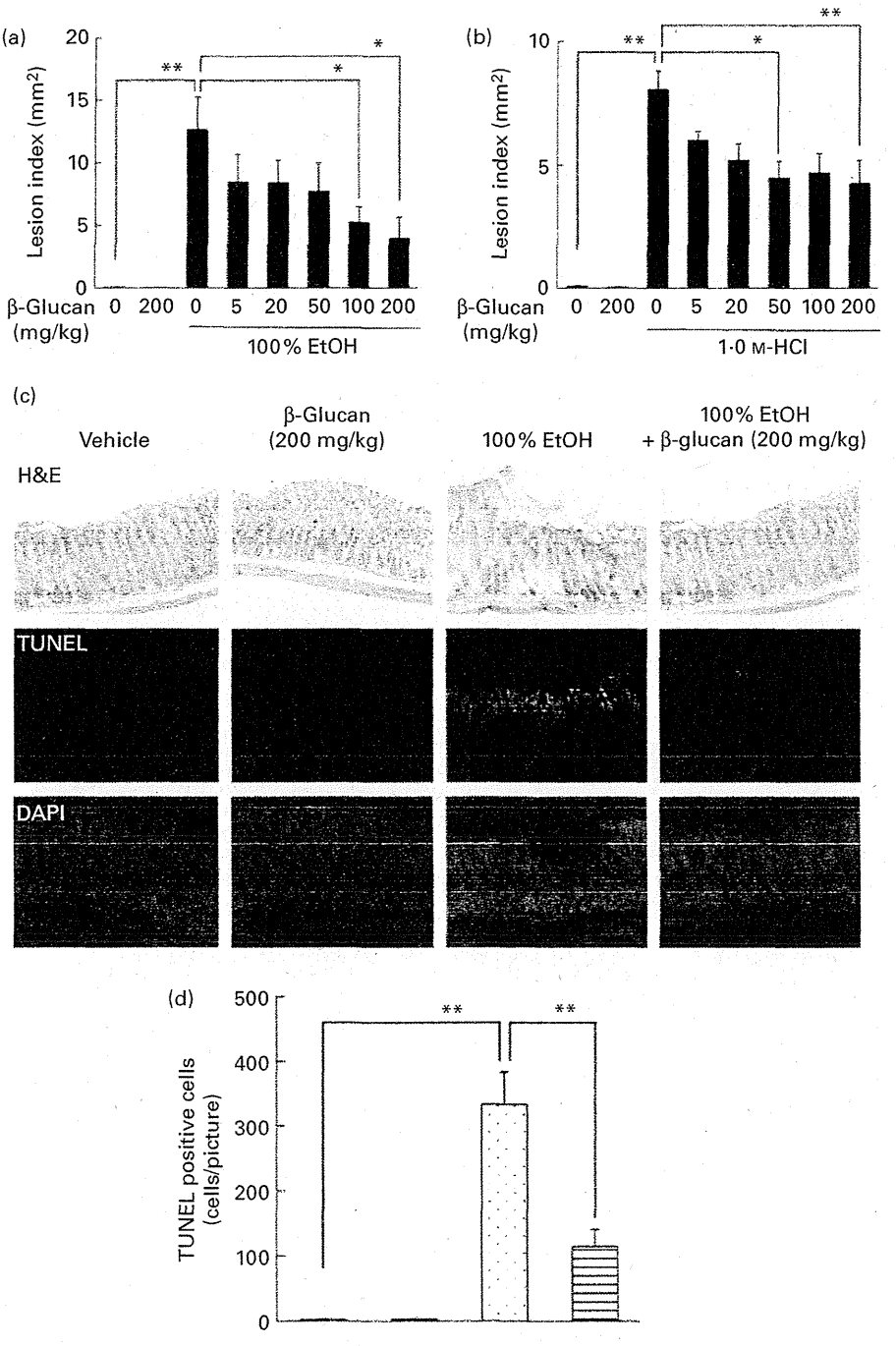

Fig. 1. Effect of low-molecular-weight β-glucan on irritant-induced gastric lesions. Mice were orally administered the indicated doses of β-glucan (mg/kg) or vehicle (□, PBS), 1 h after which they were orally administered (a, c) 100% ethanol (EtOH) (▨), (b) 1·0 M-HCl (5 ml/kg) or vehicle (water). (a, b) After 4 h, the stomach was removed and scored for haemorrhagic damage. (c) Sections of gastric tissue were prepared after 4 h and subjected to histopathological examination (haematoxylin and eosin (H&E) staining), terminal deoxynucleotidyl transferase dUTP nick-end labelling (TUNEL) assay and 4,6-diamino-2-phenylindole (DAPI) staining. (d) TUNEL-positive cells in the three sections were counted. Values are means, with their standard errors represented by vertical bars (n 3–17). Mean values were significantly different: * $P<0{\cdot}05$, ** $P<0{\cdot}01$. ■, β-Glucan (200 mg/kg); ▤, 100% EtOH + β-glucan (200 mg/kg).

British Journal of Nutrition

that oral administration of EtOH induces the expression of HSP70 in a HSF1-dependent manner, and this induction is accompanied by the production of gastric lesions[7]. As shown in Fig. 1(a), intragastric administration of 100% EtOH resulted in significant gastric lesion formation and oral pre-administration of LMW β-glucan suppressed this production in a dose-dependent manner. Oral administration of LMW β-glucan (200 mg/kg) alone did not produce gastric lesions (Fig. 1(a)). A similar protective effect of LMW β-glucan was observed for HCl-induced gastric lesions (Fig. 1(b)). Therefore, the protective effects of LMW β-glucan do not appear to be mediated in response to a specific stressor, such as EtOH. Histopathological examination by haematoxylin and eosin staining supports the notion that pre-administration of LMW β-glucan protects the gastric mucosa against EtOH-induced damage (Fig. 1(c)). Also, the level of gastric mucosal apoptosis was determined by the terminal deoxynucleotidyl transferase dUTP nick-end labelling assay. An increase in the number of terminal deoxynucleotidyl transferase dUTP nick-end labelling-positive (apoptotic) cells was observed following the administration of EtOH, and this increase was suppressed by pre-administration of LMW β-glucan (Fig. 1(c) and (d)). The results in Fig. 1 suggest that LMW β-glucan protects the gastric mucosa against irritant-induced lesions through the suppression of mucosal cell apoptosis.

Inflammatory responses, such as the infiltration of leucocytes, play an important role in the production of irritant-induced gastric lesions. In the present study, we examined the effect of LMW β-glucan on the EtOH-induced gastric

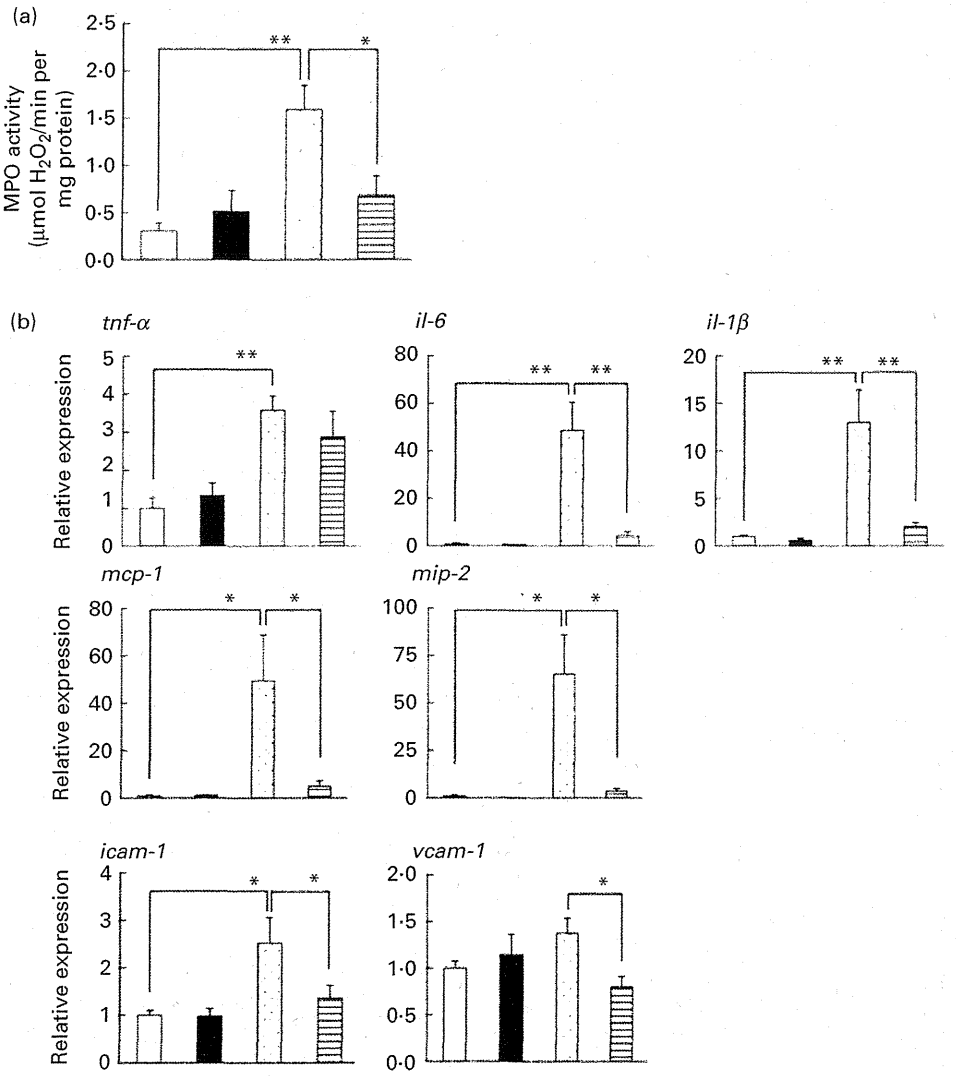

Fig. 2. Effect of low-molecular-weight β-glucan on the ethanol (EtOH)-induced gastric inflammatory response. Mice were orally administered β-glucan (■, 200 mg/kg) or vehicle (□, PBS), 1 h after which they were orally administered 100% EtOH (▤, 5 ml/kg) or vehicle (water). (a, b) After 4 h, the stomach was removed. (a) Gastric myeloperoxidase (MPO) activity was determined as described in the Materials and methods. Total RNA was extracted and subjected to real-time RT-PCR using a specific primer set for each gene. (b) Values were normalised to the *gapdh* gene and expressed relative to the control sample. Values are means, with their standard errors represented by vertical bars (n 9–14). Mean values were significantly different: * $P<0·05$, ** $P<0·01$. ▤, 100% EtOH + β-glucan (200 mg/kg). *mcp-1*, Monocyte chemoattractant protein-1; *mip-2*, macrophage inflammatory protein-2; *icam-1*, intercellular adhesion molecule-1; *vcam-1*, vascular cell adhesion molecule-1.

British Journal of Nutrition

inflammatory response by measuring gastric MPO activity, an indicator of inflammatory infiltration of neutrophils. As shown in Fig. 2(a), MPO activity increased in response to the administration of EtOH, and this increase was suppressed by pre-administration of LMW β-glucan. The administration of LMW β-glucan alone did not significantly affect the MPO activity (Fig. 2(a)).

We also examined the effects of LMW β-glucan and/or EtOH on the mRNA expression of pro-inflammatory cytokines (IL-6, IL-1β and TNF-α), chemokines (MCP-1 and MIP-2) and CAM (ICAM-1 and VCAM-1) by real-time RT-PCR analysis. As shown in Fig. 2(b), mRNA expression of all these genes except *vcam-1* was induced by EtOH administration, and this induction of the expression of all these genes except *tnf-α* was suppressed by pre-administration of LMW β-glucan. These results suggest that LMW β-glucan suppresses gastric inflammatory responses by suppressing the expression of pro-inflammatory cytokines, chemokines and CAM.

Effect of low-molecular-weight β-(1,3 → 1,6)-D-glucan on defensive factors for the gastric mucosa

In order to understand the molecular mechanism governing the protective effect of LMW β-glucan on the gastric mucosa, we examined its effect on various gastric mucosal defensive factors, such as HSP70, mucin proteins and PGE_2 *in vivo*. First, we examined the effect of LMW β-glucan and/or EtOH on HSP70 expression at the gastric mucosa by

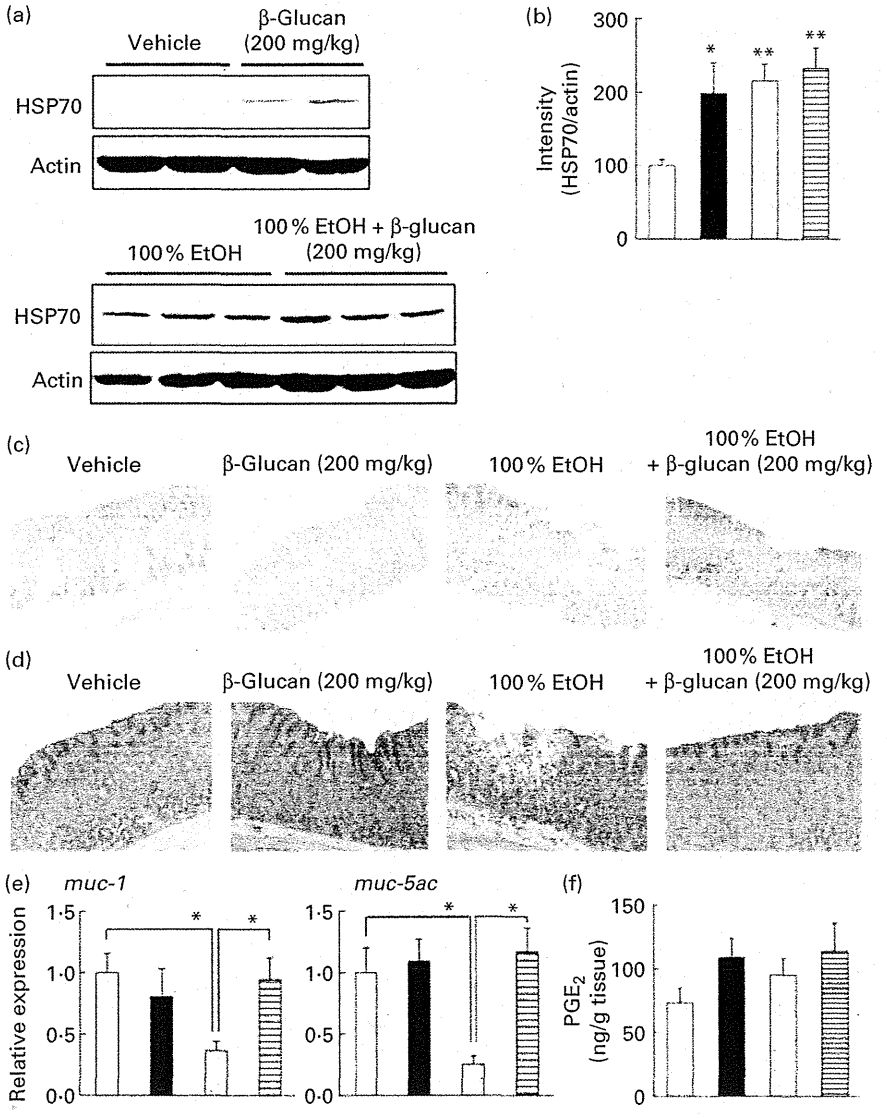

Fig. 3. Effect of low-molecular-weight β-glucan on the defensive factors for the gastric mucosa. Administration of β-glucan (■, 200 mg/kg) and 100% ethanol (EtOH, ▨) was performed as described in the legend of Fig. 2. After 4 h, the stomach was removed. (a) Total proteins were analysed by immunoblotting with an antibody against heat shock protein (HSP) 70 or actin. (b) The relative intensity of the HSP70 band to the actin band is shown (one of the gels is shown in (a)). Sections of gastric tissue were prepared and subjected to immunohistochemical analysis with an antibody against (c) HSP70 or (d) periodic acid Schiff staining. (e) The expression of mucin (*muc*)-*1* or *muc-5ac* mRNA was monitored by real-time RT-PCR, as described in the legend of Fig. 2. (f) The gastric PGE_2 level was determined by ELISA. Values are means, with their standard errors represented by vertical bars (*n* 3–9). Mean values were significantly different: * $P<0·05$, ** $P<0·01$. □, Vehicle; ▤, 100% EtOH + β-glucan (200 mg/kg).

immunoblotting analysis. As shown in Fig. 3(a) and (b), either LMW β-glucan or EtOH significantly induced the expression of HSP70. Immunohistochemical analysis supported the notions that either LMW β-glucan or EtOH induced the expression of HSP70 (Fig. 3(c)).

We also examined by periodic acid Schiff staining the effect of LMW β-glucan and/or EtOH on the level of gastric mucin. As shown in Fig. 3(d), the level of gastric mucin was reduced by the administration of EtOH, and pre-administration of LMW β-glucan restored the level. We also examined the mRNA expression of representative gastric mucin genes (*muc-1* and *muc-5ac*)[35] by real-time RT-PCR. Muc1 is a membrane-bound protein and Muc-5ac is a secreted protein[36]. As shown in Fig. 3(e), the expression of *muc-1* and *muc-5ac* mRNA was suppressed by the administration of EtOH and pre-administration of LMW β-glucan restored the expression.

The effect of LMW β-glucan and/or EtOH on gastric PGE_2 levels was also studied. As shown in Fig. 3(f), neither LMW β-glucan nor EtOH administration affected the level of PGE_2. The results in Fig. 3 suggest that LMW β-glucan protects the gastric mucosa against EtOH-induced lesions by increasing the levels of HSP70 and gastric mucin rather than that of PGE_2.

Effect of low-molecular-weight β-(1,3 → 1,6)-D-glucan on the expression of genes in vitro

In order to test whether LMW β-glucan directly affects the expression of HSP70 and mucin proteins, we examined its effect on the expression of these factors in cultured human gastric carcinoma cells. Immunoblotting analysis revealed that treatment of cells with LMW β-glucan significantly induces the expression of HSP70 in a dose-dependent manner (Fig. 4(a) and (b)).

We then examined the molecular mechanism for the LMW β-glucan-induced expression of HSP70. It is known that stressor-induced expression of HSP is mediated by the activation (phosphorylation) of HSF1. As shown in Fig. 4(c), as well as heat treatment, treatment of cells with LMW β-glucan increased the level of phosphorylated HSF1, suggesting that LMW β-glucan activates HSF1.

Previous studies have suggested that mitogen-activated protein kinases, such as p38, extracellular signal-regulated kinase and c-jun NH_2-terminal kinase, are involved in the regulation of the expression of HSP[37,38]. Therefore, we here examined the effect of inhibitors of mitogen-activated protein kinase on the LMW β-glucan-induced expression of HSP70. Pretreatment

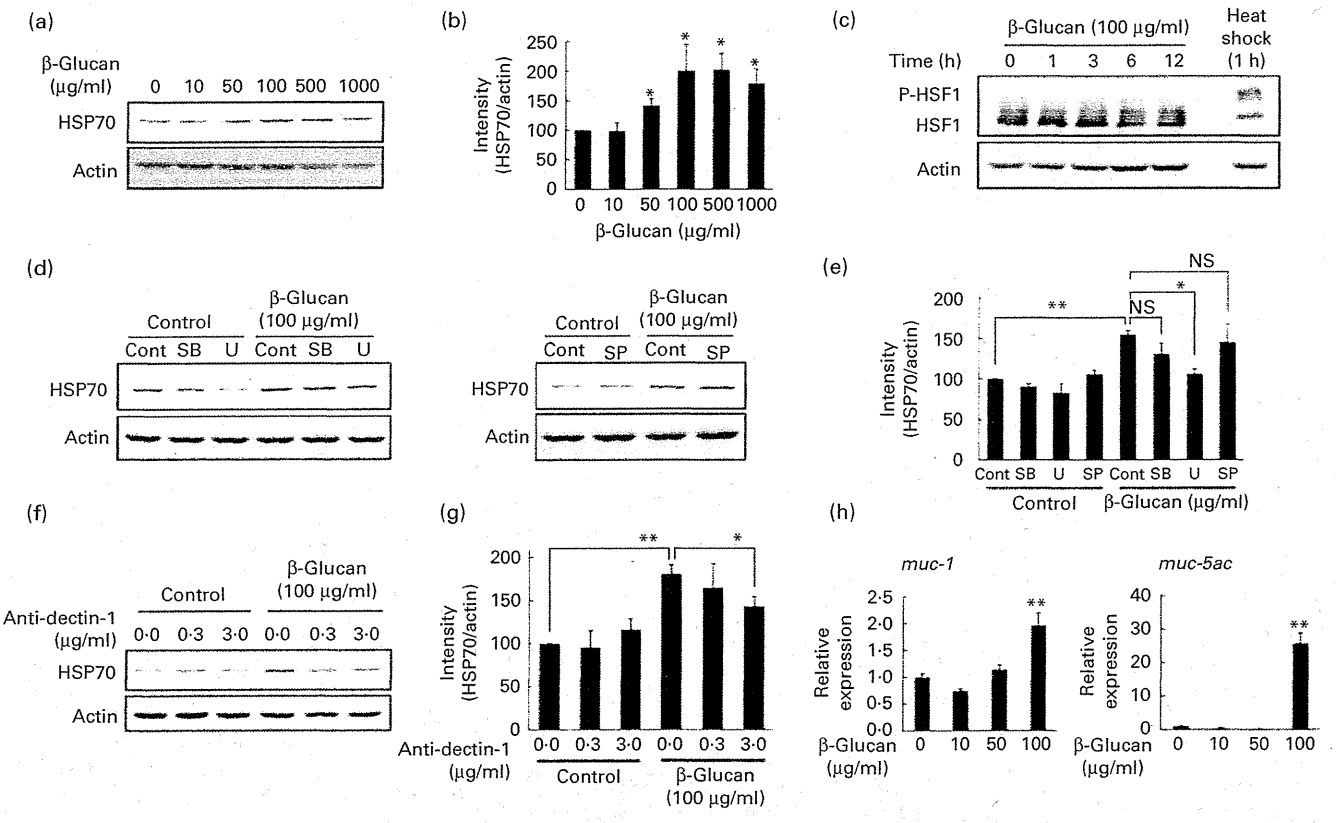

Fig. 4. Effect of low-molecular-weight (LMW) β-glucan on the expression of heat shock protein (HSP) 70 and mucin genes *in vitro*. (d, f) Human gastric carcinoma cells were pre-incubated for 1 h with or without 10 μM-SB203580 (SB), 10 μM-U0126 (U), 10 μM-SP600125 (SP) or indicated concentrations of an antibody against dectin-1. Cells were incubated with (a, h) the indicated concentrations or (c, d, f) 100 μg/ml of LMW β-glucan for (a, d, f, h) 24 h or (c) indicated periods. (c) Cells were cultured at 42°C for 1 h (heat shock). Total proteins were analysed by immunoblotting with an antibody against HSP70, heat shock factor 1 (HSF1) or actin ((a), (c), (d), (f)) (P-HSF1, phosphorylated form of HSF1). (b, e, g) The relative intensity of the HSP70 band to the actin band is shown (one of the gels is shown in (a, d, f)). The expression of mucin (*muc*)-*1* or *muc-5ac* mRNA was monitored by real-time RT-PCR, as described in the legend of Fig. 2. (h) Values were normalised to the *actin* gene. Values are means, with their standard errors represented by vertical bars (n 3–6). Mean values were significantly different: * $P<0·05$, ** $P<0·01$. cont, Control.

of cells with U0126 but not with SB203580 or SP600125 partially suppressed the LMW β-glucan-induced expression of HSP70 (Fig. 4(d) and (e)), suggesting that extracellular signal-regulated kinase is involved in the LMW β-glucan-induced expression of HSP70.

Dectin-1 was reported to be a receptor for β-glucan. In order to test the involvement of dectin-1, we examined the effect of addition of antibody against dectin-1 in the culture medium on the LMW β-glucan-induced expression of HSP70. As shown in Fig. 4(f) and (g), addition of antibody against dectin-1 in the culture medium partially suppressed the β-glucan-induced expression of HSP70, suggesting that dectin-1 is involved in the LMW β-glucan-induced expression of HSP70.

Real-time RT-PCR analysis revealed that treatment of cells with LMW β-glucan induces the expression of *muc-1* and *muc-5ac* mRNA (Fig. 4(h)).

We also examined the effect of LMW β-glucan on the lipopolysaccharide-stimulated expression of pro-inflammatory cytokines, chemokines and CAM in peritoneal macrophages prepared from mice. As shown in Fig. 5, lipopolysaccharide stimulated the mRNA expression of all these factors, and the simultaneous treatment of cells with LMW β-glucan suppressed this lipopolysaccharide-stimulated expression. The results in Figs. 4 and 5 suggest that LMW β-glucan directly affects the expression of HSP70, mucin proteins, pro-inflammatory cytokines, chemokines and CAM.

Effect of pullulan on gastric ulcerogenic response and the expression of heat shock protein 70

Since we used relatively high doses of LMW β-glucan, it may non-specifically interact with the irritants and protect the gastric mucosa. Thus, in order to test the specificity, we used another polysaccharide (α-(1,4 → 1,6)-D-glucan (pullulan)) with molecular weight similar to LMW β-glucan as the control. As shown in Fig. 6(a), oral pre-administration of pullulan (up to 200 mg/kg) did not protect the gastric mucosa against EtOH. We also examined the effect of pullulan on the expression of HSP70 both *in vivo* and *in vitro*. Oral administration of pullulan (200 mg/kg) did not increase the expression of HSP70 at the gastric mucosa with and without simultaneous administration of EtOH (Fig. 6(b) and (c)). Furthermore, treatment of human gastric carcinoma cells with pullulan (up to 1 mg/ml) did not affect the expression of HSP70 (Fig. 6(d)). Results in Fig. 6 suggest that LMW β-glucan specifically protects the gastric mucosa against irritants and induces the expression of HSP70.

Discussion

β-Glucans have been reported to have various clinically beneficial effects, such as anti-tumour effects and protective effects against bacterial, viral, fungal and parasitic challenge[9,10].

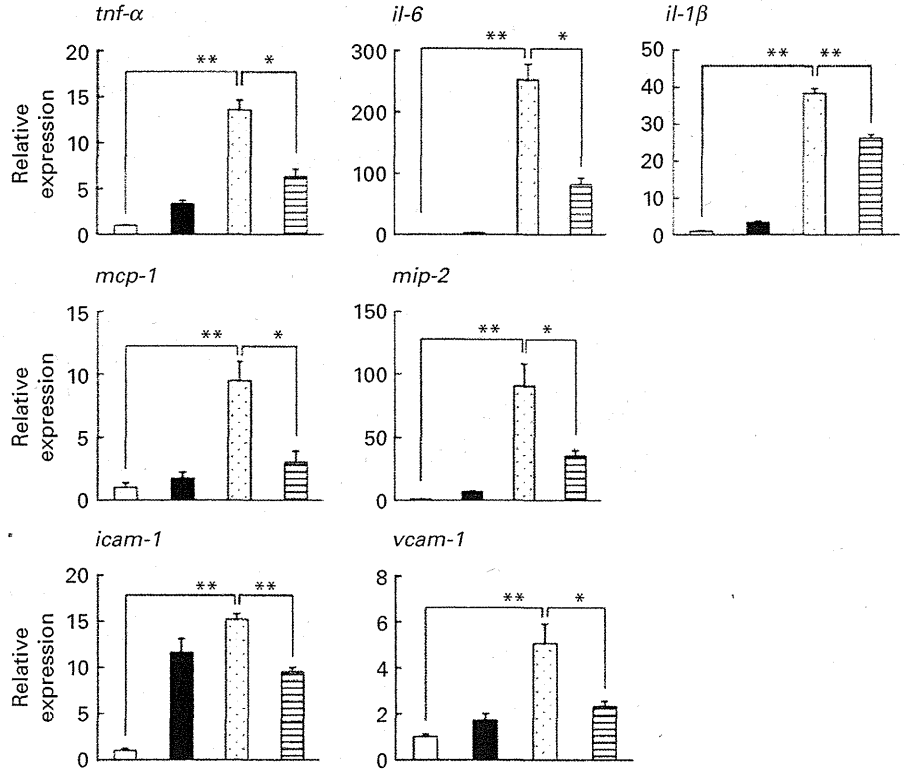

Fig. 5. Effect of low-molecular-weight β-glucan on the lipopolysaccharide (LPS)-stimulated expression of pro-inflammatory cytokines in cultured macrophages. Peritoneal macrophages were pre-incubated with β-glucan (■, 100 μg/ml) for 1 h and further incubated with LPS (▤, 1 μg/ml) for 3 h in the presence of β-glucan (100 μg/ml) as in the pre-incubation step. The expression of genes was monitored by real-time RT-PCR as described in the legend of Fig. 4. Values are means, with their standard errors represented by vertical bars (n 3–6). Mean values were significantly different: * $P<0.05$; ** $P<0.01$. □, Vehicle; ▤, LPS (1 μg/ml) + β-glucan (100 μg/ml). *mcp-1*, Monocyte chemoattractant protein-1; *mip-2*, macrophage inflammatory protein-2; *icam-1*, intercellular adhesion molecule-1; *vcam-1*, vascular cell adhesion molecule-1.

British Journal of Nutrition

Of the β-glucans, our preparation of β-(1,3)-D-glucan with β-(1,6) branches from *A. pullulans* (LMW β-glucan) is characterised by a LMW, high purity, high water solubility, low viscosity and a high level of β-(1-6) branching[14,25]. It has also been shown to have various clinically beneficial effects such as suppression of the allergic response and anti-tumour and anti-metastatic actions[14,23,25,26]. In the present study, we found another beneficial effect of LMW β-glucan, a protective effect against the formation of irritant-induced gastric lesions. Because β-glucans are known to have minimal toxic and adverse effects, we propose that β-glucans, especially LMW β-glucan, may be beneficial as health foods and supplements to prevent the formation of gastric ulcers. The findings in the present study are also important from the nutritional standpoint. Various foods, such as mushrooms, contain β-glucans. Results in the present study suggest that the intake of such foods spontaneously protects our gastric mucosa against the production of gastric lesions. Due to technical problem, we could not examine the pharmacokinetics of LMW β-glucan (such as digestion and absorption). As for other β-glucans, it has been reported that the bioavailability is from 0·5 to 5% upon oral administration[39].

Both gastric mucosal apoptosis and inflammatory responses (such as infiltration of leucocytes) play an important role in the production of irritant-induced gastric lesions, and in the present study, we have shown that both these responses are suppressed by the administration of LMW β-glucan. The anti-apoptotic effect of β-glucans has also been reported elsewhere[17,24]. On the other hand, as described earlier, β-glucans have been reported to show opposing (positive or negative) effects on immunoreactions, including inflammation. Possible explanations for this discrepancy include differences in the administration route, average molecular weight, water solubility and purity of the β-glucans employed. Another explanation is that β-glucans may have positive or negative effects on immunoreactions depending on the experimental conditions. In previous reports and in the present study, β-glucans were shown to suppress immunoreactions when the reactions were initiated by other stimuli[17–22]. On the other hand, β-glucans activate immunoreactions in intact animals[9,10,11,13]. We consider that β-glucan is a unique immunomodulator, suppressing immunoreactions when they are abnormally activated, and activating immunoreactions under normal conditions, which is important for maintaining healthy conditions.

Of the three major defensive factors for the gastric mucosa (HSP70, gastric mucin and PGE_2), we found that gastric levels of HSP70 and mucin were increased by LMW β-glucan, suggesting that these increases are responsible for the protective effect of LMW β-glucan against the formation of irritant-induced gastric lesions. We also found that EtOH-induced expression of pro-inflammatory cytokines, chemokines and CAM was suppressed by LMW β-glucan. In addition to its cytoprotective effects, the anti-inflammatory activity of HSP70 has recently been revealed; HSP70 inhibits NF-κB, which induces the expression of pro-inflammatory cytokines, chemokines and CAM[40,41]. Thus, LMW β-glucan-induced expression of HSP70 may be involved in its inhibitory

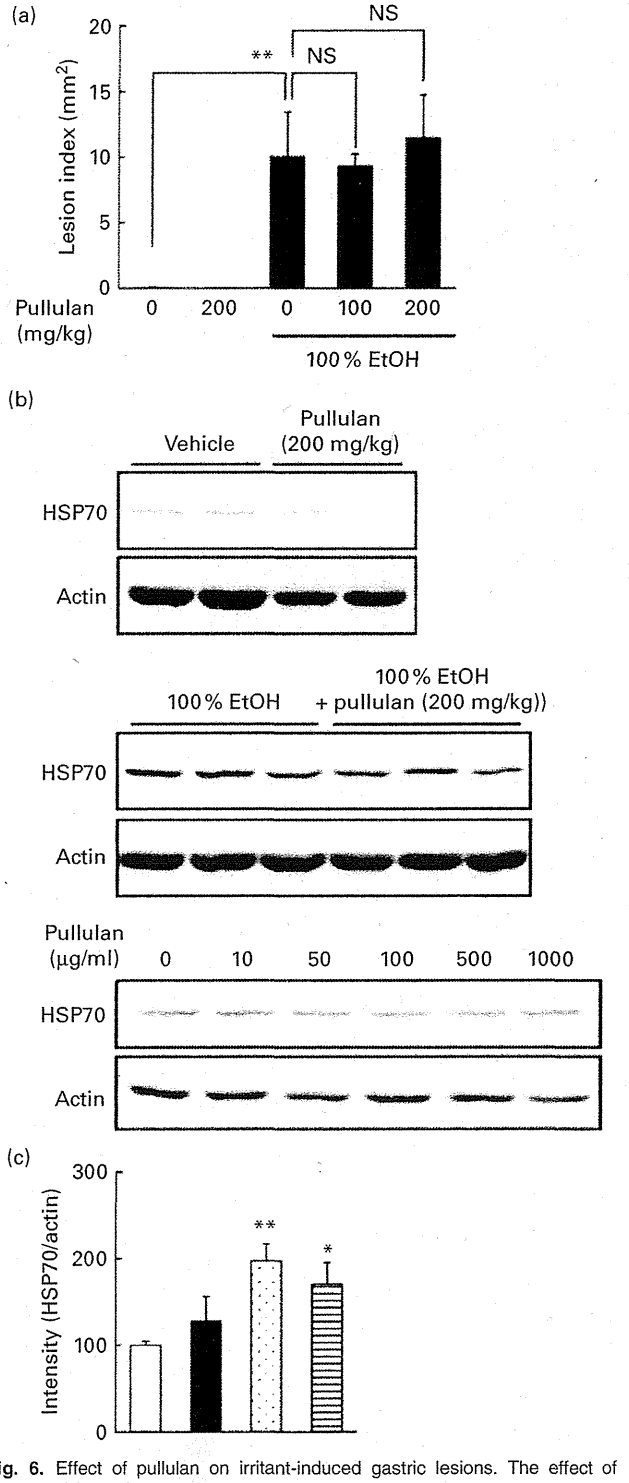

Fig. 6. Effect of pullulan on irritant-induced gastric lesions. The effect of the oral administration of pullulan on (a) ethanol (EtOH)-induced gastric lesions and (b, c) EtOH-induced expression of heat shock protein (HSP) 70 was examined as described in the legend of Figs. 1 and 3, respectively. (d) The effect of pullulan on the EtOH-induced expression of HSP70 in human gastric carcinoma cells was examined as described in the legend of Fig. 4. Values are means, with their standard errors represented by vertical bars (n 3–5). Mean values were significantly different: * $P<0·05$, ** $P<0·01$. □, Vehicle; ■, pullulan (200 mg/kg); ▦, 100% EtOH; ▤, 100% EtOH + pullulan (200 mg/kg).